Canadian Science Publishing
Canadian Journal of Fisheries and Aquatic Sciences
Journal canadien des sciences halieutiques et aquatiques

Understanding inter-reach variation in brown trout (Salmo trutta) mortality rates using a hierarchical Bayesian state-space model

Journal:	*Canadian Journal of Fisheries and Aquatic Sciences*
Manuscript ID	cjfas-2016-0240.R2
Manuscript Type:	Article
Date Submitted by the Author:	07-Jan-2017
Complete List of Authors:	BRET, Victor; EDF R&D, LNHE CAPRA, Hervé; IRSTEA, MALY GOURAUD, Véronique; EDF R&D, LNHE LAMOUROUX, Nicolas; IRSTEA, MALY Piffady, Jérémy; IRSTEA, MALY Tissot, Laurence; EDF R&D, LNHE Rivot, Etienne; Agrocampus Ouest, INRA, UMR 985 ESE Ecology and Ecosystem Health
Keyword:	Brown trout, POPULATION DYNAMICS < General, Density-dependence, spatial variation, Hierarchical Bayesien model

Understanding inter-reach variation in brown trout (*Salmo trutta*) mortality rates using a hierarchical Bayesian state-space model

Victor Bret[1], Hervé Capra[2], Véronique Gouraud[1,*], Nicolas Lamouroux[2], Jérémy Piffady[2], Laurence Tissot[1], Etienne Rivot[3]

[1] EDF R&D, LNHE Department, HYNES (Irstea – EDF R&D), 6 Quai Watier, Chatou Cedex 78401, France

[2] IRSTEA Lyon, UR MALY, HYNES (Irstea – EDF R&D), 5 Rue de la Doua, BP 32108, 69616 Villeurbanne Cedex, France

[3] UMR 985 ESE Ecology and Ecosystem Health, Agrocampus Ouest, INRA, 35042 Rennes, France

* Corresponding author

Abstract

Successful management and protection of wild animal populations relies on good understanding of their life-cycles. Because population dynamics depends on intricate interactions of biological and ecological processes at various scales, new approaches are needed that account for the variability of demographic processes and associated parameters in a hierarchy of spatial scales. A hierarchical Bayesian model for the resident brown trout (*Salmo trutta*) life cycle was built to assess the relative influence of local and general determinants of mortality. The model was fitted to an extensive data set collected in 40 river reaches, combining abundance and environmental data (hydraulics, water temperature). Density-dependent mortality of juveniles increased at low water temperatures and decreased with shelter availability. High water temperature increased density-dependent mortality in adults. The model could help to predict monthly juvenile and adult mortality under scenarios of global warming and changes in shelter availability due to habitat degradation or restoration.

Keywords

Hierarchical Bayesien model, Brown trout, population dynamics, mortality, density-dependence, spatial variation

1 Introduction

Population Dynamics Models (PDM) can capture the intricate demographic and ecological mechanisms that control the course of a population's life cycle. They contribute to decision-making for the management of fisheries (e.g., Rochette et al. 2013), invasive species (e.g., Dauer et al. 2012) or the prediction of climate change impacts (e.g., Petitgas et al. 2013). PDMs built on large scales, using data from multiple distant sites, are attractive for assessing the impact of large-scale processes such as climate patterns (e.g., Joly et al. 2011) on populations. However, local variations in population dynamics (e.g., in mortality or reproductive success; Coulson et al. 1999; Brickhill et al. 2015) can reduce the explanatory and predictive power of large-scale models that ignore variability of processes among populations. Local variations in population dynamics also threaten the transferability of PDMs calibrated locally: i.e., using extensive knowledge from monitoring one or few sites (e.g., Buenau et al. 2014). Therefore, there is a need to develop new approaches in population dynamics modeling, taking account of variability in demographic processes in a hierarchy of spatial scales to capture both patterns of variation shared by all populations and local variations, and to investigate the influence of environmental factors and anthropic pressure in a hierarchy of scales.

Hierarchical Bayesian Models (HBM) of population dynamics are useful tools to account for variability among populations (e.g., Li and Jiao 2015) due to processes operating at various scales (e.g., Ebersole et al. 2009). Moreover, HBMs can account for multiple sources of stochasticity in processes and observations, and can provide inferences on all unknowns in a full probabilistic framework (Harwood and Stokes 2003; Lek 2007; Buckland et al. 2004; Parent and Rivot 2013; Newman et al. 2014). Thus, HBMs have been widely used to model a wide range of populations (e.g., tree dynamics; McMahon et al. 2009), including age-structured (e.g., Simmonds et al. 2010; Rochette et al. 2013) or stage-structured (Swain et al. 2009) marine fish populations. However, fewer studies have used HBMs to model freshwater population dynamics (e.g., Rivot et al. 2004; Borsuk et al. 2006; Letcher et al. 2015; Kanno et al. 2016).

Brown trout (*Salmo trutta*) is one of the most widely studied freshwater fish species (Klemetsen et al. 2003) and its life-cycle has been well described (Elliott 1994; Klemetsen et al. 2003; Gouraud et al. 2014). Brown trout is typically found in headwaters, many of which have been regulated for uses such as drinking water supply and hydropower generation. Therefore, efficient management decisions require data from extensive (and expensive) long-term monitoring within a variety of headwater streams and models to predict the impact of regulations on brown trout population.

Studies explicitly comparing brown trout population dynamics among several sites are rare, but reveal considerable spatial variation. For instance, Lobón-Cerviá et al. (2012) identified differences in mortality patterns between a Spanish and a Danish population. Spatial variations were also identified among close populations (e.g., variations in competition strength and survival within a watershed; Fernandez-Chacon et al. 2015). A major source of inconsistency among studies of brown trout population dynamics lies in the identification of density-dependent mortality. This process was described theoretically a long time ago (Ricker 1954; Beverton and Holt 1957) and has been identified for all age-stages of the brown trout life cycle (Elliott 1994; Elliott and Hurley 1998; Nicola et al. 2008). However, many studies failed to detect density-dependent mortality, especially for young age-stages (Elliott and Hurley 1998; Lobón-Cerviá 2014). Such differences among studies suggest considerable spatial variation in mortality. A second source of inconsistency is due to the methods used to model environmental effects on fry mortality. Strong flow during the first months of life has frequently been related to high mortality (Hayes 1995; Cattanéo et al. 2002; Gouraud et al. 2008; Lobón-Cerviá 2014; Tissot et al. 2016), but the environmental variables used to model the process varied among studies. For instance, discharge thresholds (e.g., maximum mean daily flood) have often been used, although they correspond to very different hydraulic constraints in different rivers. Describing high flow based on standardized quantitative variables for the hydraulic habitat of brown trout (e.g., depth, velocity) might reduce these inconsistencies.

In this paper, a HBM is built to analyze resident brown trout population dynamics. The model is based on a complete representation of their life cycle, and is designed to analyze inter-reach variation in mortality to better understand the role of density-dependence. Five age-stages were distinguished, and

both density-independent and density-dependent mortality were included in the model. The model was fitted on an extensive data set collected in 40 river reaches, combining brown trout data with detailed physical habitat characteristics (e.g., hydraulics, water temperature). The reaches had a wide range of physical characteristics; half of them were below dams that diverted part of the flow. Degree of variation in mortality among reaches was quantified, and its relation with the physical characteristics of reaches was tested.

2 Materials & methods

The model was designed to capture the population dynamics of brown trout in 40 reaches of 23 rivers distributed across continental France (**Fig. 1**). Each reach included one or several sequences of pools, runs and/or riffles. Reaches had a wide range of physical characteristics (**Table 1**). They mainly comprised upstream sections of mountain streams with cold water, although three were in coastal plain streams (in Brittany and Normandy). A total of 19 reaches were below dams that diverted part of the flow (**Fig. 1**). These reaches had reduced low flows (defined by the national legislation on minimum flows) and reduced flood frequencies compared to an unregulated situation.

The model was constructed in a state-space form that included both process errors in dynamics and observation errors in data (Rivot et al. 2004; Buckland et al. 2004; Newman et al. 2014). We describe below the life-cycle model (section 2.1), the dataset used to fit the HBM and the associated observation (likelihood) equations (2.2), leave-one-out deletion tests and comparison of model fits with and without density-dependence (2.3).

2.1 The life-cycle model

The life-cycle model was based on eight demographic processes, summarized below (2.1.1) and further detailed in **Appendix A** (e.g., stage duration, equations).

2.1.1 Demographic transitions

The stage-structure PDM distinguished five age-stages (**Fig. 2**): under-gravel development (Egg), emergence (E), end of first year (0), second year (1) and adult stage (Ad). The dynamics of brown

105 trout density for a given age-stage k (D_k, ind/100m²) was modeled using 1-month time steps
106 considering different processes. The model considered eight successive processes: (p1) spawning, (p2)
107 under-gravel egg mortality, (p3) flow-velocity related mortality during emergence, mortality during:
108 (p4) emergence, (p5) end of first year (after emergence), (p6) second year of life (juvenile), and (p7)
109 the following years (**Fig. 3**). Adult mortality until spawning (p8) was also included, to predict adult
110 density at spawning, $D_{Ad,Spw}$.

111 The spawning process (p1) was described assuming that the initial egg density D_{Egg} could be related
112 to $D_{Ad,Spw}$, sex-ratio φ, number of eggs per kg of females ψ and weight (in kg) of adult brown
113 trout Kg_{Ad}.

114 Fry mortality during emergence (p3) has been reported when flow velocity was too high (e.g.,
115 Heggenes and Traaen 1988; Armstrong et al. 2003). The influence of flow velocity was therefore
116 modeled as an excess-mortality rate μ, operating when $V_{10,E}$ (daily flow velocity exceeded more than
117 10% of the time during emergence) was higher than a threshold Z (in $m.s^{-1}$). This potential abiotic
118 mortality was added to the density-dependent mortality considered in p4.

119 The 6 mortality processes (p2; p4-p8) were modeled using 1-month time steps following a Beverton-
120 Holt (1957) relationship (Quinn and Deriso 1999). This model considers both density-independent and
121 density-dependent instantaneous mortality (δ_k and γ_k respectively), assumed to be constant during the
122 whole age-stage k. The strength of both processes could therefore be studied separately. A γ_k value
123 close to 0 indicates low density-dependence for mortality. As the model assumes a closed system and
124 therefore fails to distinguish mortality from emigration, δ_k and γ_k were apparent mortality rates,
125 including both mortality as such and emigration. Instantaneous mortality rates are integrated over the
126 duration of age-stage k, Δm_k to provide the classical Beverton-Holt density-dependent relationship
127 between density at stage k and stage $k+1$:

128 (Eq.1) $$D_{k+1,m_0+\Delta m_k} = \frac{D_{k,m_0}}{e^{\delta_k.\Delta m_k} + \frac{\gamma_k}{\delta_k}.\left(e^{\delta_k.\Delta m_k}-1\right).D_{k,m_0}}$$

129 Eq. 1 can also be used to express intermediate densities within an age-stage if $\Delta m < \Delta m_k$. This was
130 used to model density at month of sampling ($D_{k_{Spl}}$) or month of spawning.

131 Process errors took account of unpredictable among-year variations around the expected process (Eq.
132 1). They were described as log-normal error, defined by its log-scale standard deviation, σ_k (estimated
133 but considered constant among reaches and years).

134 *2.1.2 Hierarchical structure and fixed parameters*

135 *2.1.2.1 Parameters fixed from the literature*

136 As we did not have local data on spawning processes and egg mortality in our reaches, parameters
137 related to these processes (p1 and p2) could not be estimated and were fixed at values from the
138 literature. We used previous studies on French brown trout populations to obtain estimates for sex-
139 ratio φ, number of eggs per kg of females ψ, and instantaneous mortality rates during the under-
140 gravel development stage δ_{Egg} and γ_{Egg} (**Table 2**). These 4 parameters were considered constant over
141 reaches and years. In particular, it was assumed that no density-dependent mortality occurred during
142 egg incubation (thus fixing γ_{Egg}=0).

143 *2.1.2.2 Parameters estimated and considered constant among reaches and years*

144 All other parameters were estimated by the model from our data and were given weakly informative
145 prior distributions (**Table 3**).

146 It was assumed that abiotic mortality (p3) could be modeled similarly in the various reaches, as a
147 function of flow velocity. Thus, μ and Z (excess-mortality rate and velocity threshold, respectively)
148 were assumed to be constant among sites and years. Inter-year variation in emergence mortality (p4) is
149 known to be high and mostly related to abiotic conditions (Hayes et al. 2010; Lobón-Cerviá et al.
150 2012). Thus, inter-reach variation was assumed to be negligible, and the parameters δ_{E} and γ_{E} were
151 considered constant among reaches.

152 As the remaining age-stages (*0*, *1* and *Ad*) were sampled, data were available to study inter-reach
153 variation in their mortality rates. An initial version of the model (online supplementary material)
154 considered inter-reach variation in all mortality rates: it revealed limited inter-reach variation in

mortality at the end of the first year (δ_0 and γ_0) and in density-independent mortality during the second year of life (δ_1). Thus, to keep the model more parsimonious, these 3 parameters were modeled as constant over reaches and years.

2.1.2.3 Parameters estimated and considered as varying among reaches

The initial version of the model indicated large inter-reach variation in mortality during the adult age-stage (δ_{Ad} and γ_{Ad}) and in density-dependent mortality during the second year of life (γ_1) (online supplementary material). These 3 parameters were therefore modeled using a hierarchical setting:

(Eq.2) $$\theta_r \sim LogN(E_\theta, \sigma_\theta)$$ (with $\theta = \delta_{\mathrm{Ad}}$, γ_1 or γ_{Ad})

enabling shared processes to be identified (expected value E_θ for parameter θ for all reaches r) while integrating reach specificities (represented by the dispersion parameter σ_θ).

2.1.3 Explaining inter-reach variation by reach characteristics

2.1.3.1 Integration of covariates in the hierarchical setting

The hypothesis that inter-reach variation in δ_{Ad}, γ_{Ad} and γ_1 could be explained by reach characteristics was further explored, focusing on 6 reach characteristics that might influence mortality: shelter availability, low and high water temperature, reach width, hydraulic suitability of habitat, and intensity of natural regime alteration (**Table 4**; data detailed in section 2.2.2). The fully exchangeable model in Eq. 2 was then extended to a partially exchangeable model (Rivot and Prévost 2002; Parent and Rivot 2013) in which the expected mean $E_{\theta,r}$ of a mortality rate θ in reach r was modelled as a linear combination of the above 6 reach characteristics:

(Eq.3) $$E_{\theta,r} = \sum_{c=1}^{6} \beta_{c,\theta} * X_{c,r} + \alpha_\theta$$

with $X_{c,r}$ the characteristic c of reach r (measured data), α_θ the intercept, and $\beta_{c,\theta}$ the slope related to characteristic c.

2.1.3.2 Identification of influential covariates

The Stochastic Search Variable Selection (SSVS) method (George and McCulloch 1993) was used to identify the most influential environmental covariates in Eq. 3. SSVS is one of several methods

developed for variable selection in Bayesian frameworks (O'Hara and Sillanpaa 2009) and has proved effective in linking fish ecology to environmental covariates (Piffady et al. 2013). The principle is to introduce latent covariates in Eq. 3, enabling variable selection to be embedded in a Markov Chain Monte Carlo (MCMC) sampling process. Eq. 3 is then extended by using auxiliary variables $I_{c,\theta}$ that indicate the presence ($I_{c,\theta}$=1) or absence ($I_{c,\theta}$=0) of covariate c for parameter θ within the model. All coefficients $\beta_{c,\theta}$ in Eq. 3 were then given a mixture prior distribution known as 'spike and slab' (George and McCulloch 1993):

(Eq.4) $$P(\beta_{c,\theta}|I_{c,\theta}) = (1 - I_{c,\theta})B0_{c,\theta} + I_{c,\theta}B1_{c,\theta}$$

The idea is to give $\beta_{c,\theta}$ a very informative prior distribution centered on 0 when $I_{c,\theta}$=0 (through $B0_{c,\theta}$), thus "turning off" the influence of this covariate. When $I_{c,\theta}$=1, then $\beta_{c,\theta}$ is given a less informative prior distribution ($B1_{c,\theta}$), likely to be updated if this covariate has an influence. Priors distributions $B1_{c,\theta}$ and $B0_{c,\theta}$ are set as Normal distributions with 0 mean and standard deviations τ and $g\tau$ respectively (g having a high positive value) (**Table 3**). As parameters τ and g needed to be tuned, we used τ=0.05 and g=500. A sensitivity analysis to test various values of τ and g (combinations of τ from 0.01 to 0.1 and g from 100 to 1,000) revealed no effect of changing those values, and will not be detailed further. Values taken by $I_{c,\theta}$ were drawn in a Bernoulli distribution with prior probability of 50% (a-priori equiprobablity of presence or absence). The posterior frequency of inclusion (i.e., number of iterations in the model with $I_{c,\theta}$=1) indicated whether factor c was likely to explain variations in the expected mean of mortality rate θ. When only low posterior frequencies of inclusion (<50%) were estimated for a given mortality rate, this indicated that the investigated reach characteristics did not explain inter-reach variation.

2.2 Data and observation equations

The PDM was fitted to annual density estimates for the various life-stages (determined by electrofishing) and to environmental variables available for the 40 reaches in the 23 rivers (**Fig. 1**).

2.2.1 *Brown trout density estimates*

2.2.1.1 *Electrofishing data*

Between 4 and 20 surveys (i.e., reach × year combinations; mean: 10.7) were conducted per reach between 1990 and 2013. Reaches were sampled by wading, using two-pass removal electrofishing sampling, meeting European Committee for Standardization guidelines (CEN 2003). At every reach r and every year y, observed brown trout densities ($D_{0_{Obs},r,y}$, $D_{1_{Obs},r,y}$ and $D_{Ad_{Obs},r,y}$) were estimated with the Carle and Strub (1978) method.

Brown trout sampling was performed without upstream or downstream blocking nets, in summer or early fall (median date: September 10). The total sampled area (between 175 and 2,902 m²) was computed as sampled length × reach width at median flow. Due to changes in sampling teams or harsh hydraulic conditions during some surveys, sampled length was slightly modified (variation >5% in measured sampled length) in 13 reaches during the study period. Such changes concerned 9% of the surveys (maximum length change: 25%; median change: 9%). The length of one reach was halved in the middle of the time series, but still considered a single reach for analysis as its hydraulic characteristics remained unchanged.

All fish were measured (total length, to the nearest 1mm), and length-frequency histograms distinguished 3 age-groups: 0+ (young-of-the-year), 1+ (between 1 and 2 years old) and adult (all fish older than two years). To confirm the suitability of using length-frequency distributions, scales were analyzed (see Sabaton et al. 2008) for 10 reaches. Adults were considered as the potential reproductive pool. Adult fish were also weighed to measure $Kg_{50,r}$, the inter-annual median of observed weights in reach r.

2.2.1.2 *Observation equations*

Sampling data ($D_{0_{Obs},r,y}$, $D_{1_{Obs},r,y}$ and $D_{Ad_{Obs},r,y}$) were observations of intermediate states of the life-cycle, occurring during processes p5, p6 and p7 respectively (**Fig. 2**; **Fig. 3**). The model predicted density at time of sampling ($D_{0_{Spl},r,y}$, $D_{1_{Spl},r,y}$ and $D_{Ad_{Spl},r,y}$), as the 1-month time-step allowed among-year variation in sampling date to be integrated. Process errors took account of unpredictable

among-year variation around the expected process (Eq. 1). Observation errors took account of uncertainty around the Carle-Strub procedure. Raw capture data were first used to calculate the relative standard deviation around the estimated density, noted as $RSD_{k,y}$ (Zippin formula; Gerdeaux 1987). Density estimates and associated uncertainty were then used as pseudo-observations in the pseudo-likelihood method (Michielsens et al. 2008). To avoid negative values, a log-normal distribution was assumed for observed densities $D_{k_{Obs},r,y}$ around $D_{k_{Spl},r,y}$ with a standard deviation in log-scale expressed by $RSD_{k,y}$.

When raw capture data were not available (11% of samples), measurement error was estimated using the 75th percentile of all RSDs.

2.2.2 Environmental data

Daily hydraulic conditions and water temperature were determined for all reaches and each year preceding fish sampling, using methods detailed by Bret et al. (2015). Daily water temperature was measured in 21 reaches (43% of the sampling period covered on average) and predictive models were used to estimate missing values. Reach-averaged hydraulic conditions (e.g., flow velocity or wetted width) were derived from daily discharge data and from numerical hydraulic models or detailed hydraulic measurements made throughout each reach at several discharge rates. Annual values of $V_{10\mathrm{E,r,y}}$ were calculated based on these data.

To test the hypothesis that inter-reach variation in mortality could be explained by reach characteristics, 6 characteristics (**Table 4**), obtained by field measurement in each reach r, were selected and standardized before being introduced in the model. Shelter availability ($Shelt_r$) was described as the ratio of sheltered area (under a rock or the bank) to total wetted area. The mean of annual percentiles of water temperatures ($T_{10,r}$ and $T_{90,r}$) was used to summarize the extreme range of thermal regimes. The mean of annual median wetted widths ($L_{50,r}$) was used to describe stream size. Habitat suitability was described by the Habitat Suitability Index at median discharge ($HSI_{50,r}$), calculated using the instream habitat models of Lamouroux and Capra (2002) (28 reaches), Sabaton and Miquel (1993) (5 reaches) or Ginot et al. (1998) (7 reaches) depending on available data. The

256 strength of natural regime alteration was represented by the height of the nearest upstream dam
257 ($hDam_r$).

258 *2.2.3 MCMC simulations*

259 Posterior distributions were inferred via MCMC sampling using JAGS software (information at
260 http://mcmc-jags.sourceforge.net) and the R package R2jags (Plummer et al. 2015). Three independent
261 MCMC chains were run, starting at different random initial values. After a "burn-in" period of 80,000
262 iterations, 3 × 40,000 iterations were sampled, 1 in 10 being recorded to reduce sampling
263 autocorrelation. The Gelman-Rubin diagnostic (Brooks and Gelman 1998) was used to test for chain
264 convergence (Gelman-Rubin statistics <1.1).

265 *2.3 Model stability and comparison with a model without density-dependence*

266 Leave-one-out deletion tests were used to estimate the reliability of the SSVS and sensitivity of
267 parameter estimates to small changes in data. The model was fitted on 40 different subsets of 39
268 reaches (leaving out 1 reach in turn per subset). Posterior frequencies for inclusion of reach
269 characteristics were compared to assess SSVS stability. Posterior means of all parameters' posterior
270 distributions were also compared to evaluate the stability of parameter estimates.

271 Finally, to assess the consequences of integrating density-dependence, the model including the
272 environmental variables selected by the SSVS procedure was compared to a model with all density-
273 dependent mortality rates set to 0 (only density independent mortality). The explanatory power of the
274 two models was compared, based on their log-scaled Root Mean Square Error (RMSE) computed as
275 $\sqrt{\frac{1}{n}\sum_{i=1}^{n}(\log(D_{Spl,k,i}) - \log(D_{Obs,k,i}))^2}$ for each of the three sampled age-stages k, where $D_{Spl,k,i}$ is
276 the fitted density and $D_{Obs,k,i}$ is the pseudo-observation.

3 Results

3.1 Explaining mortality variation by reach characteristics

Inter-reach variation was found for density-independent mortality for the adult age-stage δ_{Ad} and density-dependent mortality for the 1+ and adult age-stages (γ_1 and γ_{Ad}; see online supplementary material). The SSVS revealed that, of the 6 reach-specific characteristics, only shelter availability and water temperature explained these inter-reach variations (**Fig. 4A**). There was an influence of reach shelter availability ($Shelt$) on density-dependent mortality for the 1+ age-stage (γ_1) (posterior frequency of inclusion = 85%; **Fig. 4A**), describing decreasing density-dependence with shelter availability (mean value of posterior PDF of $\beta_{Shelt,\gamma_1} = -1.2$; **Table 5**; **Fig. 5**, second row). Density-dependent mortality for the 1+ age-stage (γ_1) was also increased by low water temperatures (T_{90}; posterior frequency of inclusion = 70%; **Fig. 4A**; **Table 5**; **Fig. 5**, third row). There was finally an influence of high water temperatures (T_{10}) on density-dependent mortality for the adult age-stage (γ_{Ad}) (posterior frequency of inclusion = 74%; **Fig. 4A**), describing increasing density-dependence with high water temperature (mean value of posterior PDF of $\beta_{T_{10},\gamma_{Ad}} = 0.3$; **Table 5**; **Fig. 5**, fourth row). No reach characteristics significantly explained the variations in adult density-independent mortality (δ_{Ad}; **Fig. 5**, first row).

These results were confirmed by the leave-one-out deletion tests (**Fig. 4B**). The posterior frequency of inclusion of $Shelt$ (influencing γ_1), T_{90} (influencing γ_1) or T_{10} (influencing γ_{Ad}) remained >50% in respectively 100%, 92.5% and 97.5% of the cases. The influence of high water temperature on adult density-dependent mortality appeared strong (**Fig. 5**, fourth row) when considering all reaches. However, one deletion test (removal of the Clarée reach) showed surprising results for adults: inter-reach variation in γ_{Ad} was explained by shelter availability (posterior frequency of inclusion when removing the Clarée reach= 71%) rather than by high water temperatures (posterior frequency of inclusion of T_{10} = 35%). This reach exhibited low shelter availability ($Shelt_{Clarée}$= 0.6%), low water temperatures ($T_{10,Clarée}$=12°C) and low density-dependent mortality for the adult ($\gamma_{Ad,Clarée}$=0.003) and induced a bias in our results. Other variables that were removed from the model (influence of

303 reach width, habitat suitability or natural regime alteration on $\delta_{Ad}, \gamma_1, \gamma_{Ad}$ and of thermal regime and
304 shelter availability on δ_{Ad}) always showed the lowest probability of inclusion (<42%).

305 *3.2 Variations in mortality according to age-stage*

306 Monthly mortality differed widely among age-stages (**Table 5**). The lowest were $\delta_0, \delta_1, \gamma_0$ (posterior
307 means always <0.001) and $\gamma_{1,r}$ (posterior means <0.002 for 24 reaches; max: 0.038) (**Fig. 6**). Other
308 monthly mortality rates were much higher. The highest mortality occurred during emergence
309 (posterior mean of δ_E=0.24, γ_E=0.02). Estimates of δ_E revealed a wide uncertainty (50% of the
310 posterior PDF within [0.12; 0.33]). The posterior means of the 40 fitted $\delta_{Ad,r}$s ranged between 0.003
311 and 0.160 (mean: 0.014) and posterior means of the $\gamma_{Ad,r}$s ranged between 0.002 and 0.026 (mean:
312 0.010).

313 The posterior distributions of parameters showing high flow influence on recruitment (μ and Z; **Table**
314 **5**) revealed very high mortality in emerging fry (94%; posterior mean of μ) for flow velocity ($V_{10E,r,y}$)
315 >1.15m.s^{-1} (posterior mean of Z). Extreme mortality was therefore modeled for only 8% of studied
316 years. Combined with the high density-dependent mortality during emergence γ_E, this produced
317 estimates of 0+ density very stable among reaches (see **Fig. 7**, right panel), associated with high
318 process error.

319 *3.3 Comparing observed and predicted density*

320 The model was indeed able to predict temporal change in 1+ and adult density (see **Fig. 7** for an
321 example of 2 reaches), but often overlooked 0+ temporal density variation. This was quantified by the
322 posterior mean of the RMSE for these age groups (1.23.1, 0.72 and 0.50 for 0+, 1+ and adults
323 respectively). The high values of posterior PDF for $\sigma_0, \sigma_1, \sigma_{Ad}$ revealed a considerable influence of
324 process error: real density in 50% of samplings was within a range of [0.5*$D_{0_{Spl}}$ – 2.0*$D_{0_{Spl}}$] for 0+,
325 [0.6*$D_{1_{Spl}}$ – 1.5*$D_{1_{Spl}}$] for 1+ and [0.8*$D_{Ad_{Spl}}$ – 1.3*$D_{Ad_{Spl}}$] for adults.

3.4 Stability of the model and comparison with a model without density-dependence

Results of the leave-one-out deletion test showed that inferences were fairly robust with respect to moderate changes within data sets. The relative standard deviations on the study parameters were always <10%. RMSE was also very stable (<2.5% variation) for all age-stages, showing that the quality of fit of the model to the data was not dependent on any data in particular.

By contrast, a priori setting all density-dependent parameters to 0 and estimating density-independent mortality only decreased the explanatory power of the model, as log-scale RMSE values were higher (1.40, 0.82 and 0.54 for 0+, 1+ and adults, corresponding to respective increases of 14%, 14% and 8%), showing that density-dependence was important in explaining the data.

4 Discussion

4.1 Fitting the brown trout life-cycle

The extensive dataset analyzed in this study enabled construction of a hierarchical Bayesian state-space model for the life-cycle of resident brown trout. While previous attempts to model brown trout life-cycle used no or few data (e.g., Van Winkle et al. 1998; Daufresne and Renault 2006) or adopted a deterministic approach with literature-based parameters (e.g., Railsback et al. 2009; Tissot et al. 2016), our population dynamics model is merged within a statistical approach in which most state variables and parameters were estimated from field data, accounting for both process and observation errors (Rivot et al. 2004; Buckland et al. 2007; Parent and Rivot 2013).

Posterior distributions of mortality estimated on our 40 reaches were consistent with values reported in the literature. High mortality during emergence (p4) has long been reported (e.g., between 85% and 98% of mortality occurred during emergence for the 4 years studied by Elliott 1994). The present pattern of low mortality during age-stages 0 and 1 (p5 and p6) was also identified by samplings made every 2 months on two Spanish reaches for 11 and 14 years by Lobón-Cerviá (2012). Mean annual adult mortality at mean adult density (53%; **Fig. 6** p7) was consistent with previous reports (50%; Baglinière and Maisse 1991), but ranged between 20% at low density and 80% at high density.

Results, based on long term monitoring of 40 reaches, confirmed that density-dependence is a major feature of brown trout population dynamics. Indeed, integrating density-dependent mortality (γ) into natural mortality processes (p2; p4-p8) improved the explanatory power of the model. Wide variations were identified in the strength of density-dependence among reaches (**Fig. 6**): annual mortality of juveniles (p6) and adults (p7) could vary 2-fold for a given initial density of 1+ or adults, only due to variations in γ.

4.2 Inter-reach variation in mortality

Results revealed a high variability of survival across reaches. Contrasting reaches distributed across France and exhibiting a wide range of physical characteristics (**Table 2**) were included in the analysis. While some mortality rates were very stable across all reaches (δ_0, γ_0 and δ_1), inter-reach variations were identified, even among geographically close populations, for γ_1, δ_{Ad} and γ_{Ad}. Spatial variation in density-dependent mortality was mostly explained by 3 reaches characteristics: shelter availability and inter-annual quantiles describing extreme water temperatures (T_{10} and T_{90}). In line with studies by Myrvold and Kennedy (2015) on steelhead self-thinning, the present results suggest that the strength of density-dependence is predictable from habitat characteristics.

4.2.1 Shelter availability reduces the strength of density-dependence

The clearest explanation of variation in density-dependence was increasing density-dependent mortality for the 1+ age-stage with decreasing shelter availability. Most γ_1 values were low but increased when the reach had less than 2% of its area available as shelter, with maximal values when nearly no sheltered area was available (**Fig. 5**). A similar trend appeared to drive γ_{Ad} when one reach was removed. Future research should then also consider the influence of shelter availability on density-dependent mortality for the adult age-stage. The impact of shelter availability on mortality was previously reported in many papers, for brown trout (Armstrong et al. 2003; Dieterman and Hoxmeier 2011) or other salmonids (Finstad et al. 2007), and was used in the individual-based model developed by Van Winkle et al. (1998). The present results were also consistent with those reported by Baran (1995), who identified a decrease in maximal juvenile and adult brown trout density with decreasing shelter availability (especially below 2% availability).

4.2.2 *Thermal regime influences the strength of density-dependence*

Density-dependent mortality for 1+ brown trout increased for the lowest water temperature (T_{90}<4°C). By contrast, density-dependent mortality for adult brown trout seemed to increase with high water temperature (**Fig. 5**). This might explain why 1+ density-dependent mortality was more often found in northern (e.g., Vøllestad and Olsen 2008) than in southern streams (e.g., Lobón-Cerviá 2012). Studies conducted in southern streams clearly identified density-dependence in adults (Lobón-Cerviá 2012). The higher fitted values for γ_{Ad} compared to γ_1 also explained why this process was easier to observe in previous studies. Temperature influence on density dependence may be explained by its effects on metabolism (Elliott 1976; Coutant 1976), swimming performance (Railsback et al. 2009) and foraging efficiency (Watz and Piccolo 2011). For example, swimming speed varies non-linearly with temperature, peaking at temperatures around a median temperature range of about 15°C (Railsback et al. 2009). We also suggested that higher water temperature might increase the activity of adult brown trout, leading to aggressive territorial behaviors.

4.2.3 *Understanding inter-reach variation in δ_{Ad}*

We were not able to explain the observed inter-reach variation in adult density-independent mortality (δ_{Ad}). However, variation in this parameter (**Fig. 5**, first row) was largely driven by 2 reaches with exceptionally high posterior estimates (posterior means of δ_{Ad}>0.05), while most reaches presented lower estimates (33 reaches showed posterior means < 0.015). The two outlying reaches were distant from each other and had different physical characteristics (a wide natural reach draining 250 km² and a reach below a dam, draining only 9 km²). Inter-reach variation in δ_{Ad} might then result from factors that were not monitored, such as a contrast in angling pressure or variation in population dynamics induced by removal of individuals (Almodovar and Nicola 2004).

4.2.4 *Reach characteristics unrelated to change in mortality*

The weak effect of habitat sustainability index (HSI) was to be expected, as HSI was designed to predict aggregate indicators of fish population status (biomass, or carrying capacity) rather than specific demographic processes (Hayes et al. 2009). While position in the stream network was previously used as an indicator of the suitability of a reach for a specific species or age-stage (e.g.,

Chaumot et al. 2003), median width was unrelated to mortality in the present data. Finally, the height (and thus presence) of an upstream dam did not affect mean mortality processes downstream. When dams have existed for decades, it is likely that populations have adapted to the conditions induced by the dam. Moreover, many features of population dynamics other than mortality were not studied here, and might be influenced by the presence of an upstream dam (e.g., access to suitable spawning areas, sensitivity to environmental conditions).

4.3 Limitations of our modeling approach and possible extension

The present model focused on density-dependence and inter-reach variation in mortality. However, more processes could easily be added to the model. Hierarchical Bayesian modeling is especially suited to combining varied sources of information and sub-models (e.g., following Lecomte and Laplanche 2012 or Rochette et al. 2013). Therefore, it is important to identify which key processes could be integrated in the present model to enhance its ecological realism.

4.3.1 Adding abiotic processes

The present model included abiotic 0+ mortality linked to flow velocity during emergence (p3), which captured rare extreme mortality events. However, consistently with the literature showing that variations in 0+ density is mainly driven by intricate combinations of environmental conditions (e.g., Unfer et al. 2011; Lobón-Cerviá 2014), our model revealed a very low predictive power of 0+ density (high process stochasticity in 0+, seen through σ_0). Analysis of temporal variation in 0+ density would likely be improved by modeling additional abiotic processes of direct mortality. For example, including frequency or duration of high or low flows (Lobón-Cerviá 2009) or streambed mobility (Unfer et al. 2011; Bret et al. 2015) could improve modeling of 0+ density. Abiotic processes used in other modeling approaches, such inSTREAM (Railsback et al. 2009; e.g., direct influence of high temperature or reduced habitat availability) or MODYPOP (Gouraud et al. 2008; e.g., direct influence of flushing or high-flow in periods other than emergence), could also be considered.

429 *4.3.2 Modeling growth and movement*

430 Beyond these additional influences, considering processes such as growth or movement would consist
431 in interesting future research avenues. Because growth and survival are linked, adding growth
432 dynamics would likely improve the comprehension of brown trout population dynamics (e.g., Ebersole
433 et al. 2009; Nislow and Armstrong 2012).

434 The present model considered all reaches as closed systems, although downstream drift of young
435 individuals (Daufresne et al. 2005) and upstream migration of spawners (Young et al. 2010; Vøllestad
436 et al. 2012) have been reported for brown trout. Consequently, the present mortality estimates covered
437 both actual mortality and displacement. For instance, low mortality during the first year of life might
438 be linked to partial replacement of dead individuals by migrants from upstream or tributaries, and may
439 hide a complex source-sink dynamic among reaches. Modeling movement is challenging. One
440 approach could be to integrate individual mark-recapture data in the population dynamics model
441 through an integrated population model (Schaub et al. 2007; Schaub and Abadi 2011; Letcher et al.
442 2015). However, movement can be complicated by reach characteristics such as degree of longitudinal
443 connectivity (presence of a dam or natural barrier, configuration of tributaries).

444 *4.3.3 Improving the representation of mortality during emergence*

445 Available data do not allowed us to model the variation of mortality during emergence among reaches.
446 Additional information on spawning and emergence processes (e.g., local observations of fecundity
447 according to spawner mass, frequent evaluation of recruits' survival) would help modeling variations
448 among reaches.

449 *4.3.4 Modeling variation in stage duration among populations*

450 Contrary to Lobón-Cerviá et al. (2012) who suggested that the number and duration of age-stages
451 might differ among populations, the number and duration of the processes underlying the life-cycle
452 were assumed equal for all populations in our model. The 3 reaches located in Brittany and Normandy
453 presented very different physical characteristics (e.g., smaller streambed particles, lower elevation and
454 higher water temperature), and would likely have different dynamics as the other reaches.
455 Accordingly, previous comparisons among brown trout populations from Brittany and the Pyrenees

456 mountains (Gouraud et al. 2001) revealed that brown trout tended to be larger and shorter-lived in
457 Brittany. However, these populations did not appear as outliers in the present data, and were well
458 integrated in the hierarchical model: the differences in juvenile and adult mortality were explained by
459 their reach characteristics. Nonetheless, 0+ densities were over-estimated for these 3 reaches,
460 confirming differences in spawning and early-life processes.

461

462 Integration of density-dependence is crucial to explaining juvenile and adult mortality, especially
463 where little shelter is available in a reach. The results also highlighted the influence of water
464 temperature on density-dependence strength. The model could help to predict change in monthly
465 mortality in juveniles and adults under scenarios of global warming and changes in shelter availability
466 due to habitat degradation or restoration (example for mean initial densities: **Fig. 8**). For instance, an
467 increase in density (stocking) might not result in a long-term increase in population level in
468 unfavorable reaches (low shelter availability), due to strong density-dependent mortality. Increasing
469 available shelter area is, on the other hand, likely to reduce competition among juveniles and increase
470 population levels. With further developments, the present model might become a useful tool to help
471 management decision-making, to test scenarios in natural and regulated reaches. It will, however, be
472 necessary to enhance the model's ability to capture temporal variations before considering predictions.

473 # 5 Acknowledgement

474 We thank the numerous people (working at ONEMA, Electricité de France, IRSTEA, ECOGEA,
475 angling associations and other consulting firms) who contributed to electrofishing and habitat
476 measurements. We also thank the organizations which provided environmental data (ONEMA, Météo
477 France, and angling associations).

478

6 References

Almodovar, A., and Nicola, G.G. 2004. Angling impact on conservation of Spanish stream-dwelling brown trout Salmo trutta. Fisheries Management and Ecology **11**(3-4): 173-182.

Armstrong, J.D., Kemp, P.S., Kennedy, G.J.A., Ladle, M., and Milner, N.J. 2003. Habitat requirements of Atlantic salmon and brown trout in rivers and streams. Fish. Res. **62**(2): 143-170.

Baglinière, J.L., and Maisse, G. 1991. La truite - Biologie et écologie. INRA Editions.

Baran, P. 1995. Analyse de la variablité des abondances de truites communes (*Salmo trutta* L.) dans les Pyrénées centrales françaises.

Bardonnet, A., and Prévost, E. 1994. Survie sous gravier de la truite (*Salmo trutta*) dans un affluent du Scorff. Internal report, AIP Eau, INRA Rennes.

Beverton, R.J.H., and Holt, S.J. 1957. On the dynamics of exploited fish populations. Chapman & Hall, London, UK.

Borsuk, M.E., Reichert, P., Peter, A., Schager, E., and Burkhardt-Holm, P. 2006. Assessing the decline of brown trout (*Salmo trutta*) in Swiss rivers using a Bayesian probability network. Ecological Modelling **192**(1-2): 224-244.

Bret, V., Bergerot, B., Capra, H., Gouraud, V., and Lamouroux, N. 2015. Influence of discharge, hydraulics, water temperature and dispersal on density synchrony in brown trout populations (*Salmo trutta*). Can. J. Fish. Aquat. Sci. **73**(3): 319-329.

Brickhill, D., Evans, P.G.H., and Reid, J.M. 2015. Spatio-temporal variation in European starling reproductive success at multiple small spatial scales. Ecology and Evolution **5**(16): 3364-3377.

Brooks, S.P., and Gelman, A. 1998. General Methods for Monitoring Convergence of Iterative Simulations. Journal of Computational and Graphical Statistics **7**(4): 434-455.

Buckland, S.T., Newman, K.B., Fernandez, C., Thomas, L., and Harwood, J. 2007. Embedding Population Dynamics Models in Inference. 44-58.

Buckland, S.T., Newman, K.B., Thomas, L., and Koesters, N.B. 2004. State-space models for the dynamics of wild animal populations. Ecological Modelling **171**(1–2): 157-175.

Buenau, K.E., Hiller, T.L., and Tyre, A.J. 2014. Modelling the effects of river flow on population dynamics of piping plovers (*Charadrius melodu*) and least terns (*Sternula antillarum*) nesting on the Missouri river. River. Res. Applic. **30**(8): 964-975.

Caissie, D. 2006. The thermal regime of rivers: a review. Freshw. Biol. **51**(8): 1389-1406.

Carle, R.T., and Strub, M.R. 1978. A new method for estimating population size from removal data. Biometrics **34**(4): 621-630.

Cattanéo, F., Lamouroux, N., Breil, P., and Capra, H. 2002. The influence of hydrological and biotic processes on brown trout (*Salmo trutta*) population dynamics. Can. J. Fish. Aquat. Sci. **59**: 12-22.

CEN. 2003. Water quality – sampling of fish with electricity. European Standard.

Chaumot, A., Charles, S., Flammarion, P., and Auger, P. 2003. Ecotoxicology and spatial modeling in population dynamics: An illustration with brown trout. Environmental Toxicology and Chemistry **22**(5): 958-969.

Coulson, T., Albon, S., Pilkington, J., and Clutton-Brock, T. 1999. Small-scale spatial dynamics in a fluctuating ungulate population. J. Anim. Ecol. **68**(4): 658-671.

Coutant, C.C. 1976. Thermal effects on fish ecology. *In* Encyclopedia of Environmental Science and Engineering. Gordon and Breach Publishers. pp. 891-896.

Dauer, J.T., McEvoy, P.B., and Van Sickle, J. 2012. Controlling a plant invader by targeted disruption of its life cycle. Journal of Applied Ecology **49**(2): 322-330.

Daufresne, M., Capra, H., and Gaudin, P. 2005. Downstream displacement of post-emergent brown trout: effects of development stage and water velocity. J. Fish Biol. **67**(3): 599-614.

Daufresne, M., and Renault, O. 2006. Population fluctuations, regulation and limitation in stream-living brown trout. Oikos **113**(3): 459-468.

Dieterman, D.J., and Hoxmeier, R.J.H. 2011. Demography of Juvenile and Adult Brown Trout in Streams of Southeastern Minnesota. Trans. Am. Fish. Soc. **140**(6): 1642-1656.

529 Dunbar, M.J., Alfredsen, K., and Harby, A. 2012. Hydraulic-habitat modelling for setting
530 environmental river flow needs for salmonids. Fisheries Management and Ecology **19**(6): 500-517.
531 Ebersole, J.L., Colvin, M.E., Wigington, P.J., Leibowitz, S.G., Baker, J.P., Church, M.R., Compton, J.E.,
532 and Cairns, M.A. 2009. Hierarchical Modeling of Late-Summer Weight and Summer Abundance of
533 Juvenile Coho Salmon across a Stream Network. Trans. Am. Fish. Soc. **138**(5): 1138-1156.
534 Elliott, J.A., and Hurley, M.A. 1998. Population regulation in adult, but not juvenile, resident trout
535 (Salmo trutta) in a Lake District stream. J. Anim. Ecol. **67**(2): 280-286.
536 Elliott, J.M. 1976. The Energetics of Feeding, Metabolism and Growth of Brown Trout (Salmo trutta
537 L.) in Relation to Body Weight, Water Temperature and Ration Size. J. Anim. Ecol. **45**(3): 923-948.
538 Elliott, J.M. 1994. Quantitative ecology and the brown trout. Oxford University Press, Oxford GBR.
539 Fernandez-Chacon, A., Genovart, M., Alvarez, D., Cano, J.M., Ojanguren, A.F., Rodriguez-Munoz, R.,
540 and Nicieza, A.G. 2015. Neighbouring populations, opposite dynamics: influence of body size and
541 environmental variation on the demography of stream-resident brown trout (Salmo trutta).
542 Oecologia **178**(2): 379-389.
543 Finstad, A.G., Einum, S., Forseth, T., and Ugedal, O. 2007. Shelter availability affects behaviour, size-
544 dependent and mean growth of juvenile Atlantic salmon. Freshw. Biol. **52**(9): 1710-1718.
545 George, E.I., and McCulloch, R.E. 1993. Variable Selection via Gibbs Sampling. Journal of the
546 American Statistical Association **88**(423): 881-889.
547 Ginot, V., Souchon, Y., Capra, H., Breil, P., and Valentin, S. 1998. Logiciel EVHA 2.0. Evaluation de
548 l'habitat physique des poissons en rivière. Cemagref BEA/LHQ et Ministère de l'Aménagement du
549 Territoire et de l'Environnement.
550 Gouraud, V., Baglinière, J.L., Baran, P., Sabaton, C., Lim, P., and Ombredane, D. 2001. Factors
551 regulating brown trout populations in two french rivers: Application of a dynamic population model.
552 Regul. River. **17**: 557-569.
553 Gouraud, V., Baran, P., Bardonnet, A., Beaufrère, C., Capra, H., Caudron, A., Delacoste, M., Lescaux,
554 J.M., Naura, M., Ovidio, M., Poulet, N., Tissot, L., Sebaston, C., and Baglinière, J.-L. 2014. Sur quelles
555 connaissances se baser pour évaluer l'état de santé des populations de truite commune (*Salmo*
556 *trutta*)? Hydroécologie Appliquée: 1-28.
557 Gouraud, V., Capra, H., Sabaton, C., Tissot, L., Lim, P., Vandewalle, F., Fahrner, G., and Souchon, Y.
558 2008. Long-term simulations of the dynamics of trout populations on river reaches bypassed by
559 hydroelectric installations—analysis of the impact of different hydrological scenarios. River. Res.
560 Applic. **24**(9): 1185-1205.
561 Harwood, J., and Stokes, K. 2003. Coping with uncertainty in ecological advice: lessons from fisheries.
562 Trends in Ecology & Evolution **18**(12): 617-622.
563 Hayes, D., Jones, M., Lester, N., Chu, C., Doka, S., Netto, J., Stockwell, J., Thompson, B., Minns, C.,
564 Shuter, B., and Collins, N. 2009. Linking fish population dynamics to habitat conditions: insights from
565 the application of a process-oriented approach to several Great Lakes species. Rev Fish Biol Fisheries
566 **19**(3): 295-312.
567 Hayes, J.W. 1995. Spatial and temporal variation in the relative density and size of juvenile brown
568 trout in the Kakanui River, North Otago, New Zealand. New Zeal. J. Mar. Fresh. **29**(3): 393-407.
569 Hayes, J.W., Olsen, D.A., and Hay, J. 2010. The influence of natural variation in discharge on juvenile
570 brown trout population dynamics in a nursery tributary of the Motueka River, New Zealand. New
571 Zeal. J. Mar. Fresh. **44**(4): 247-269.
572 Heggenes, J. 1996. Habitat selection by brown trout (*Salmo trutta*) and young atlantic salmon (*S.*
573 *salar*) in streams : Static and dynamic hydraulic modelling. Regul. River. **12**(2-3): 155-169.
574 Heggenes, J., and Traaen, T. 1988. Downstream migration and critical water velocities in stream
575 channels for fry of four salmonid species. J. Fish Biol. **32**(5): 717-727.
576 Joly, K., Klein, D.R., Verbyla, D.L., Rupp, T.S., and Chapin, F.S. 2011. Linkages between large-scale
577 climate patterns and the dynamics of Arctic caribou populations. Ecography **34**(2): 345-352.
578 Kanno, Y., Pregler, K.C., Hitt, N.P., Letcher, B.H., Hocking, D.J., and Wofford, J.E.B. 2016. Seasonal
579 temperature and precipitation regulate brook trout young-of-the-year abundance and population
580 dynamics. Freshw. Biol. **61**(1): 88-99.

Keith, P., Persat, H., Feunteun, E., and Allardi, J. 2011. Les Poissons d'eau douce de France.
Klemetsen, A., Amundsen, P.A., Dempson, J.B., Jonsson, B., Jonsson, N., O'Connell, M.F., and Mortensen, E. 2003. Atlantic salmon *Salmo salar* L., brown trout *Salmo trutta* L. and Arctic charr *Salvelinus alpinus* (L.): a review of aspects of their life histories. Ecol. Freshw. Fish **12**: 1-59.
Lamouroux, N., and Capra, H. 2002. Simple predictions of instream habitat model outputs for target fish populations. Freshw. Biol. **47**: 1543–1556.
Lecomte, J.-B., and Laplanche, C. 2012. A length-based hierarchical model of brown trout (*Salmo trutta fario*) growth and production. Biometrical Journal **54**(1): 108-126.
Lek, S. 2007. Uncertainty in ecological models. Ecological Modelling **207**(1): 1-2.
Letcher, B.H., Schueller, P., Bassar, R.D., Nislow, K.H., Coombs, J.A., Sakrejda, K., Morrissey, M., Sigourney, D.B., Whiteley, A.R., O'Donnell, M.J., and Dubreuil, T.L. 2015. Robust estimates of environmental effects on population vital rates: an integrated capture-recapture model of seasonal brook trout growth, survival and movement in a stream network. J Anim Ecol **84**(2): 337-352.
Li, Y., and Jiao, Y. 2015. Evaluation of stocking strategies for endangered white abalone using a hierarchical demographic model. Ecological Modelling **299**: 14-22.
Lobón-Cerviá, J. 2009. Why, when and how do fish populations decline, collapse and recover? The example of brown trout (*Salmo trutta*) in Rio Chaballos (northwestern Spain). Freshw. Biol. **54**(6): 1149-1162.
Lobón-Cerviá, J. 2012. Density-dependent mortality in adults, but not juveniles, of stream-resident brown trout (*Salmo trutta*). Freshw. Biol. **57**(10): 2181-2189.
Lobón-Cerviá, J. 2014. Recruitment and survival rate variability in fish populations: density-dependent regulation or further evidence of environmental determinants? Can. J. Fish. Aquat. Sci. **71**(2): 290-300.
Lobón-Cerviá, J., Budy, P., and Mortensen, E. 2012. Patterns of natural mortality in stream-living brown trout (*Salmo trutta*). Freshw. Biol. **57**(3): 575-588.
Lobon-Cervia, J., and Rincon, P.A. 2004. Environmental determinants of recruitment and their influence on the population dynamics of stream-living brown trout *Salmo trutta*. Oikos **105**(3): 641-646.
McMahon, S.M., Dietze, M.C., Hersh, M.H., Moran, E.V., and Clark, J.S. 2009. A Predictive Framework to Understand Forest Responses to Global Change. Annals of the New York Academy of Sciences **1162**(1): 221-236.
Michielsens, C.G.J., McAllister, M.K., Kuikka, S., Mäntyniemi, S., Romakkaniemi, A., Pakarinen, T., Karlsson, L., and Uusitalo, L. 2008. Combining multiple Bayesian data analyses in a sequential framework for quantitative fisheries stock assessment. Can. J. Fish. Aquat. Sci. **65**(5): 962-974.
Myrvold, K.M., and Kennedy, B.P. 2015. Local habitat conditions explain the variation in the strength of self-thinning in a stream salmonid. Ecology and Evolution **5**(16): 3231-3242.
Newman, K., Buckland, S.T., Morgan, B., King, R., Borchers, D.L., Cole, D., Besbeas, P., Gimenez, O., and Thomas, L. 2014. Modelling Population Dynamics. Springer-Verlag New York.
Nicola, G.G., Almodóvar, A., Jonsson, B., and Elvira, B. 2008. Recruitment variability of resident brown trout in peripheral populations from southern Europe. Freshw. Biol. **53**(12): 2364-2374.
Nislow, K.H., and Armstrong, J.D. 2012. Towards a life-history-based management framework for the effects of flow on juvenile salmonids in streams and rivers. Fisheries Management and Ecology **19**(6): 451-463.
O'Hara, R.B., and Sillanpaa, M.J. 2009. A review of Bayesian variable selection methods: what, how and which. 85-117.
Parent, E., and Rivot, E. 2013. Introduction to Hierarchical Bayesian Modeling for Ecological Data. Chapman and Hall/CRC
Petitgas, P., Rijnsdorp, A.D., Dickey-Collas, M., Engelhard, G.H., Peck, M.A., Pinnegar, J.K., Drinkwater, K., Huret, M., and Nash, R.D.M. 2013. Impacts of climate change on the complex life cycles of fish. Fisheries Oceanography **22**(2): 121-139.

631 Piffady, J., Parent, É., and Souchon, Y. 2013. A hierarchical generalized linear model with variable
632 selection: studying the response of a representative fish assemblage for large European rivers in a
633 multi-pressure context. Stoch Environ Res Risk Assess **27**(7): 1719-1734.
634 Plummer, M., Stukalov, A., and Denwood, M. 2015. rjags 3-15.
635 Poff, L.N., Olden, J.D., Merritt, D.M., and Pepin, D.M. 2007. Homogenization of regional river
636 dynamics by dams and global biodiversity implications. Proc Natl Acad Sci U S A **104**(14): 5732-5737.
637 Quinn, T.J., and Deriso, R.B. 1999. Quantitative fish dynamics. Oxford University Press, New York.
638 Railsback, S.F., Harvey, B.C., Jackson, S.K., and Lamberson, R.H. 2009. InSTREAM: the individual-based
639 stream trout research and environmental assessment model. Gen. Tech. Rep., Albany, CA: U.S.
640 Department of Agriculture, Forest Service, Pacific Southwest Research Station.
641 Ricker, W.E. 1954. Stock and Recruitment. Journal of the Fisheries Research Board of Canada **11**(5):
642 559-623.
643 Rivot, E., and Prévost, E. 2002. Hierarchical Bayesian analysis of capture-mark-recapture data. Can. J.
644 Fish. Aquat. Sci. **59**(11): 1768-1784.
645 Rivot, E., Prévost, E., Parent, E., and Baglinière, J.L. 2004. A Bayesian state-space modelling
646 framework for fitting a salmon stage-structured population dynamic model to multiple time series of
647 field data. Ecological Modelling **179**(4): 463-485.
648 Rochette, S., Le Pape, O., Vigneau, J., and Rivot, E. 2013. A hierarchical Bayesian model for
649 embedding larval drift and habitat models in integrated life cycles for exploited fish. Ecol. Appl. **23**(7):
650 1659-1676.
651 Sabaton, C., and Miquel, J. 1993. La méthode des micro-habitats : un outil d'aide au choix d'un débit
652 réservé à l'aval des ouvrages hydroélectriques. Expérience d'Electricité de France. Hydroécologie
653 appliquée **5**(1): 127-163
654 Sabaton, C., Souchon, Y., Capra, H., Gouraud, V., Lascaux, J.M., and Tissot, L. 2008. Long-term brown
655 trout populations responses to flow manipulation. River. Res. Applic. **24**(5): 476-505.
656 Schaub, M., and Abadi, F. 2011. Integrated population models: a novel analysis framework for deeper
657 insights into population dynamics. Journal of Ornithology **152**(S1): 227-237.
658 Schaub, M., Gimenez, O., Sierro, A., and Arlettaz, R. 2007. Use of Integrated Modeling to Enhance
659 Estimates of Population Dynamics Obtained from Limited Data. Conservation Biology **21**(4): 945-955.
660 Simmonds, E.J., Portilla, E., Skagen, D., Beare, D., and Reid, D.G. 2010. Investigating agreement
661 between different data sources using Bayesian state-space models: an application to estimating NE
662 Atlantic mackerel catch and stock abundance. ICES Journal of Marine Science: Journal du Conseil
663 **67**(6): 1138-1153.
664 Swain, D.P., Jonsen, I.D., Simon, J.E., and Myers, R.A. 2009. Assessing threats to species at risk using
665 stage-structured state–space models: mortality trends in skate populations. Ecol. Appl. **19**(5): 1347-
666 1364.
667 Tharme, R.E. 2003. A global perspective on environmental flow assessment : emerging trends in the
668 development and application of environmental flow methodologies for rivers. River. Res. Applic. **19**:
669 397-441.
670 Tissot, L., Bret, V., Capra, H., Baran, P., and Gouraud, V. 2016. Main potential drivers of trout
671 population dynamics in bypassed stream sections. Ecol. Freshw. Fish.
672 Unfer, G., Hauer, C., and Lautsch, E. 2011. The influence of hydrology on the recruitment of brown
673 trout in an Alpine river, the Ybbs River, Austria. Ecol. Freshw. Fish **20**(3): 438-448.
674 Van Winkle, W., Jager, Y., and Holcomb, B. 1998. An individual-based model for sympatric
675 populations of brown and rainbow trout. Oak ridge national laboratory, Oak ridge.
676 Vøllestad, L.A., and Olsen, E.M. 2008. Non-additive effects of density-dependent and density-
677 independent factors on brown trout vital rates. Oikos **117**(11): 1752-1760.
678 Vøllestad, L.A., Serbezov, D., Bass, A., Bernatchez, L., Olsen, E.M., and Taugbøl, A. 2012. Small-scale
679 dispersal and population structure in stream-living brown trout (Salmo trutta) inferred by mark–
680 recapture, pedigree reconstruction, and population genetics. Can. J. Fish. Aquat. Sci. **69**(9): 1513-
681 1524.

682 Watz, J., and Piccolo, J.J. 2011. The role of temperature in the prey capture probability of drift-
683 feeding juvenile brown trout (Salmo trutta). Ecol. Freshw. Fish **20**(3): 393-399.
684 Young, R.G., Hayes, J.W., Wilkinson, J., and Hay, J. 2010. Movement and mortality of adult brown
685 trout in the Motupiko River, New Zealand: effects of water temperature, flow, and flooding. Trans.
686 Am. Fish. Soc. **139**(1): 137-146.

687

688 7 Tables

689 ***Table 1.*** *Physical characteristics of the 40 stream reaches.*

Physical characteristics	Min	Mean	Max
Width at median discharge L_{50} (m)	2.9	8.1	15.5
Reach slope (%)	0.3	3.3	13.2
Elevation (m)	15.0	814.1	1370.0
Distance from source (km)	3.0	17.6	49.0
Basin area (km²)	9.0	131.5	605.0
Median daily discharge Q_{50} ($m^3.s^{-1}$)	0.1	1.0	2.8
Reach flow velocity ($m.s^{-1}$) at Q_{50}	0.1	0.4	0.8
Median daily water temperature T_{50} (°C)	5.8	8.1	11.3
Shelter availability (% of the total wetted area)	0.27	2.21	6.45
Habitat Suitability Index (0+ and 1+ brown trout) at Q_{50}	0.2	0.4	0.7
Habitat Suitability Index (adult brown trout) at Q_{50}	0.0	0.2	0.4

690
691

692 ***Table 2.*** *Fixed values and tight informative priors for parameters used in the model (LogN= Log-Normal*
693 *distribution)*

Parameter	Definition	Source	Prior distribution
φ	Sex-ratio	Lobon-Cervia and Rincon 2004; Gouraud et al. 2014	Beta(200,200)
ψ	Fecundity (eggs.kg^{-1})	Keith et al. 2011; Gouraud et al. 2008; Gouraud et al. 2014	Log-N(7.6, 0.005)
δ_{Egg}	Density-independent mortality rate during egg incubation	Bardonnet and Prévost 1994	Beta(15,370)
γ_{Egg}	Density-dependent mortality rate during egg incubation	Gouraud et al. 2014; Bardonnet and Prévost 1994	Fixed to 0

694

695

696 ***Table 3.*** *Definitions, related equations and prior distributions of all parameters for which updating was*
697 *expected from the data. Indices k denote age-stages, c denote reach characteristics*
698 *(c= T_{50}, L_{50}, $Shelt$, HSI, $hBarr$; parameters defined in **Table 4**) and θ denotes parameters dependent on hyper-*
699 *parameters (N=Normal distribution; LogN=Log-Normal distribution).*

Parameter	Definition	Related process / equation	Prior distribution
Global parameters			
μ	Excess-mortality rate induced by flow velocity >Z during emergence (m.s^{-1})	p3	Beta(1,1)
Z	Threshold for flow-velocity mortality during emergence (m.s^{-1})	p3	Gamma(1,1)
δ_k	Global instantaneous density-independent mortality rate	p2 (k=Egg) p4 (k=E) p5 (k=0) p6 (k=1)	LogN(0,1)
γ_k	Global instantaneous density-dependent mortality rate	p4 (k=E) p5 (k=0)	LogN(0,1)
σ_k	Process stochasticity	(k=0, 1, Ad)	Gamma(1,1)
Hyper-parameters			
$\beta_{\theta,c}$	Slope of the link between E_θ (expected mean of parameter θ) and reach characteristic c	Eq. 3 (θ=$\gamma_1, \delta_{Ad}, \gamma_{Ad}$)	See Eq. 4
$I_{c,\theta}$	Auxiliary variable indicating whether covariate c has an influence ($I_{c,\theta}$=1) or not ($I_{c,\theta}$=0) on parameter θ	Eq. 4 (θ=$\gamma_1, \delta_{Ad}, \gamma_{Ad}$)	Bernoulli(0.5)
$B0_{c,\theta}$	'Spike' of the mixture distribution of $\beta_{\theta,c}$ (used when $I_{c,\theta}$=0)	Eq. 4 (θ=$\gamma_1, \delta_{Ad}, \gamma_{Ad}$)	N(0,τ)
$B1_{c,\theta}$	'Slab' of the mixture distribution of $\beta_{\theta,c}$ (used when $I_{c,\theta}$=1)	Eq. 4 (θ=$\gamma_1, \delta_{Ad}, \gamma_{Ad}$)	N(0,$g\tau$)
α_θ	Intercept for E_θ	Eq. 3 (θ=$\gamma_1, \delta_{Ad}, \gamma_{Ad}$)	N(-1,2)
σ_θ	Standard deviation for parameter θ	Eq. 2 (θ=$\gamma_1, \delta_{Ad}, \gamma_{Ad}$)	Gamma(1,1)
Parameters θ dependent on hyper-parameters			
δ_k	Hierarchical instantaneous density-independent mortality rate	p7 & p8 (k=Ad)	LogN($E_{\delta_k}, \sigma_{\delta_k}$)
γ_k	Hierarchical instantaneous density-dependent mortality rate	p6 (k=1) p7 & p8 (k=Ad)	LogN($E_{\gamma_k}, \sigma_{\gamma_k}$)

700

701 **Table 4.** *Reach characteristics used for the SSVS. The influence of the chosen proxies on inter-reach differences*
702 *in mortality rates were tested.*

Characteristics (Notation)	Rationale	Details
Shelter availability ($Shelt_r$)	Brown trout are known to seek shelter (Heggenes 1996; Klemetsen et al. 2003). Positive influence of shelter has been identified on salmonid growth and mortality (Finstad et al. 2007; Dieterman and Hoxmeier 2011).	Ratio of sheltered area to total wetted area (in %). Sheltered area = recorded area (to the nearest 15 cm²) of all areas greater than 200 cm², located under the river bank or streambed rock
Water temperature ($T_{10,r}$ and $T_{90,r}$)	Thermal regime might indirectly influence mortality through changes in dissolved oxygen concentration or growth (Caissie 2006). We chose to summarize extreme values.	Mean of annual percentiles values (temperatures exceeded 10 and 90% of the time; in °C).
Reach width ($L_{50,r}$)	Brown trout are known to live in small mountain (or coastal) streams (Keith et al. 2011). Thus, information on reach width might help easily predict the reach's suitability for brown trout (seen here as apparent mortality rates)	Mean of annual median wetted width. $L_{50,r}$ was correlated with distance from source ($\rho = 0.72$) and drainage basin area ($\rho = 0.69$).
Habitat suitability ($HSI_{50,r}$)	Potential available habitat within the reach might also influence apparent mortality. The Habitat Suitability Index (HSI) considers 3 habitat components (depth, velocity and substrate size) and predicts the evolution of the potential habitat with discharge (e.g., Tharme 2003; Dunbar et al. 2012).	HSI at median discharge ($HSI_{50,r}$) for both younger age-stages (0+ and 1+) and adult brown trout in every reach, following Lamouroux and Capra 2002.
Natural regime alteration ($hDam_r$)	The presence of a dam induces changes downstream (e.g., reduced food drift from upstream, reduced sediment transport; Poff et al. 2007). These changes, increasing with the size of the dam, might induce differences in mortality below dams.	Height of the nearest upstream dam (in m): if no dam upstream, set at 0.

703

704 ***Table 5.*** *Main statistics of the marginal posterior distributions for the parameters estimated across all reaches*

705 *and years.*

Process	Parameter	Mean	2.5%	25%	Median	75%	97.5%
p1	ψ	1,993	1,734	1,900	1,989	2,086	2,278
	φ	0.50	0.45	0.48	0.50	0.52	0.55
p2	δ_{Egg}	0.04	0.02	0.03	0.04	0.05	0.06
p3	μ	0.94	0.85	0.93	0.95	0.96	0.98
	Z	1.15	1.10	1.14	1.15	1.17	1.21
p4	δ_E	0.24	0.04	0.12	0.21	0.33	0.62
	γ_E	0.02	0.01	0.02	0.02	0.03	0.03
p5	δ_0	2.67E-03	1.00E-03	1.86E-03	2.50E-03	3.30E-03	5.24E-03
	γ_0	1.22E-03	5.73E-04	9.54E-04	1.19E-03	1.45E-03	2.02E-03
p6	δ_1	2.95E-03	1.09E-03	2.07E-03	2.77E-03	3.64E-03	5.78E-03
	α_{γ_1}	-6.94	-8.15	-7.23	-6.88	-6.58	-6.10
	$\beta_{\gamma_1,Shelt}$	-1. 21	-2.40	-1.62	-1.30	-1.04	-0.61
	$\beta_{\gamma_1,\mathrm{T90}}$	-0.60	-1.48	-0.93	-0.70	-0.50	-0.12
	σ_{γ_1}	0.98	0.36	0.75	0.95	1.17	1.74
p7, p8	$\alpha_{\delta_{Ad}}$	-5.47	-7.32	-5.97	-5.37	-4.88	-4.16
	$\sigma_{\delta_{Ad}}$	1.62	0.87	1.26	1.54	1.89	2.78
	$\alpha_{\gamma_{Ad}}$	-4.84	-5.12	-4.93	-4.84	-4.75	-4.59
	$\beta_{\gamma_{Ad},\mathrm{T10}}$	0.35	0.08	0.24	0.32	0.40	0.56
	$\sigma_{\gamma_{Ad}}$	0.59	0.37	0.51	0.59	0.67	0.85
Process Stochasticity	σ_0	1.05	0.98	1.02	1.05	1.07	1.12
	σ_1	0.63	0.58	0.61	0.63	0.64	0.67
	σ_{Ad}	0.41	0.38	0.39	0.40	0.42	0.44

706
707

8 Figures

Fig. 1. *Locations of the 40 reaches (19 below dams).*

Fig. 2. *Life-cycle model for resident brown trout (S. trutta), split into 5 stages (Egg: eggs; E: emergent fry; 0: juvenile during the end of the first year; 1: 1+; Ad: adults) and 8 processes (black arrows) related to model equations (Appendix A). Gray boxes show the dates of transition between stages, set at the 15th day of the month (3: March, 5: May, 12: December) of the year indicated in subscript (starting year y = spawning year). Other subscripts denote spawning (Spw), initial state of an age-stage (i), and integrated mortality due to flow velocity (V) or sampling (Spl). The population was observed at sampling (during p5, p6 and p7). Adults (Ad) age-stage combined fish of several ages (2: fish in their 3rd year of life, >2: fish older than 3 years).*

Fig. 3. *Directed acyclic graph for the brown trout population dynamics model presented in Fig. 1. Variables represented in ellipses were defined by a probability distribution. White ellipses are non-observed variables; shaded ellipses are data. Shaded boxes represent fixed constant or calculated covariates. Solid-line arrows represent stochastic transitions; dotted-line arrows represent deterministic links (including age-stage transitions, structuring the life-cycle). The number of each process (p1 – p8; detailed in Appendix A) is added.*

Fig. 4. *Posterior frequency of inclusion (in %) of the effect of the 6 studied reach characteristics (rows) on the 3 mortality rates (columns). Table A shows the results of the model for the 40 reaches. Table B summarizes the results of the leave-one-out deletion test, giving median [range] values for posterior frequency of inclusion. Gray scale is associated with the posterior frequency of inclusion.*

Fig. 5. *Marginal posterior distributions of density-independent (δ_{Ad}) and density-dependent (γ_1 and γ_{Ad}) mortality rates modeled by a hierarchical structure for the 40 reaches. The 1st row shows the distribution of δ_{Ad}, which could not be explained by reach characteristics. The 2nd to 5th rows show change in density-dependent mortality distribution (γ_1 and γ_{Ad}) with shelter availability and inter-annual mean of percentile of water temperatures (T_{10} and T_{90}) as covariates.*

Fig. 6. *Total mortality for the processes describing natural mortality between successive age-stages (p4, p5, p6 and p7) for total process duration (respectively, 2, 10, 12 and 12 months). When inter-reach variation in at least one mortality rate (δ_k or γ_k) was detected for age-stage k, fitted relations for the 40 reaches are presented (dashed gray lines) along with the mean expected relation (solid line). A vertical line is drawn at mean observed densities for 0+, 1+and adults (densities were never observed at emergence); upper limits of x-axes correspond to the 90th percentile of observed densities. Mortality from egg to emergent fry is not represented here, as mortality rates were not fitted but taken from the literature.*

Fig. 7. *Time series of observed and predicted densities of 0+, 1+ and adult brown trout in 2 reaches (Bes and Senouire; columns). Points represent observed densities, associated with observation uncertainty (vertical lines). The black line shows the mean estimate of each year's predicted density. The shaded areas show the 50% and 95% confidence intervals for the predicted densities, when process error is considered.*

Fig. 8. *Prediction of monthly mortality in 1+ depending on shelter availability (x-axis) and inter-annual mean of a percentile of water temperatures (T_{90}) (y-axis). Black dots show the characteristics of reaches considered in this paper. Marginal relations are shown in upper and right sub-panels (shaded areas show 50% and 95% confidence intervals). Monthly mortality was computed by considering both density-independent and density-dependent mortality and for mean initial densities (10.5 ind.100m^{-2} for 1+ and 8.1 ind.100m^{-2} for adults).*

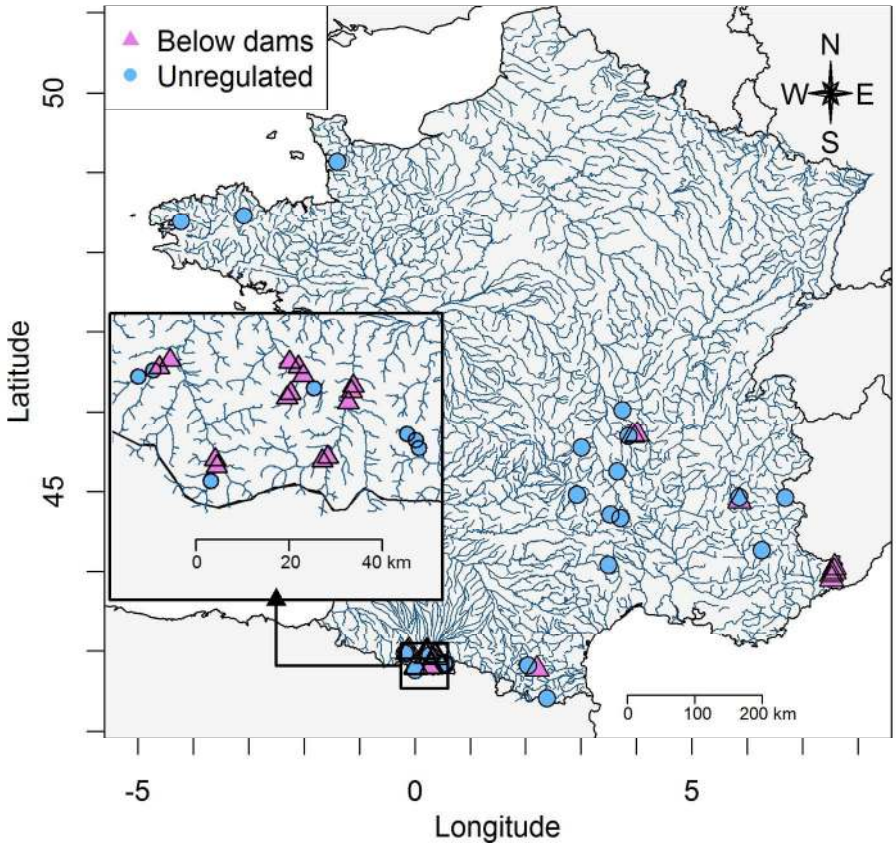

Locations of the 40 reaches (19 below dams).

169x159mm (300 x 300 DPI)

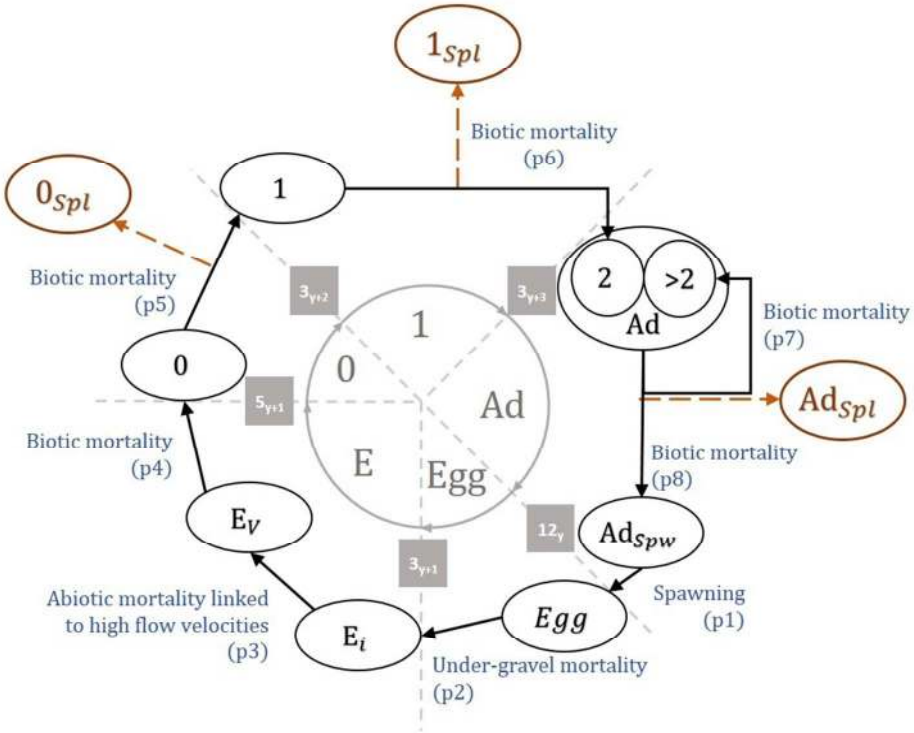

Fig. 2. Life-cycle model for resident brown trout (S. trutta), split into 5 stages (Egg: eggs; E: emergent fry; 0: juvenile during the end of the first year; 1: 1+; Ad: adults) and 8 processes (black arrows) related to model equations (Appendix A). Gray boxes show the dates of transition between stages, set at the 15th day of the month (3: March, 5: May, 12: December) of the year indicated in subscript (starting year y = spawning year). Other subscripts denote spawning (Spw), initial state of an age-stage (i), and integrated mortality due to flow velocity (V) or sampling (Spl). The population was observed at sampling (during p5, p6 and p7). Adults (Ad) age-stage combined fish of several ages (2: fish in their 3rd year of life, >2: fish older than 3 years).

289x220mm (96 x 96 DPI)

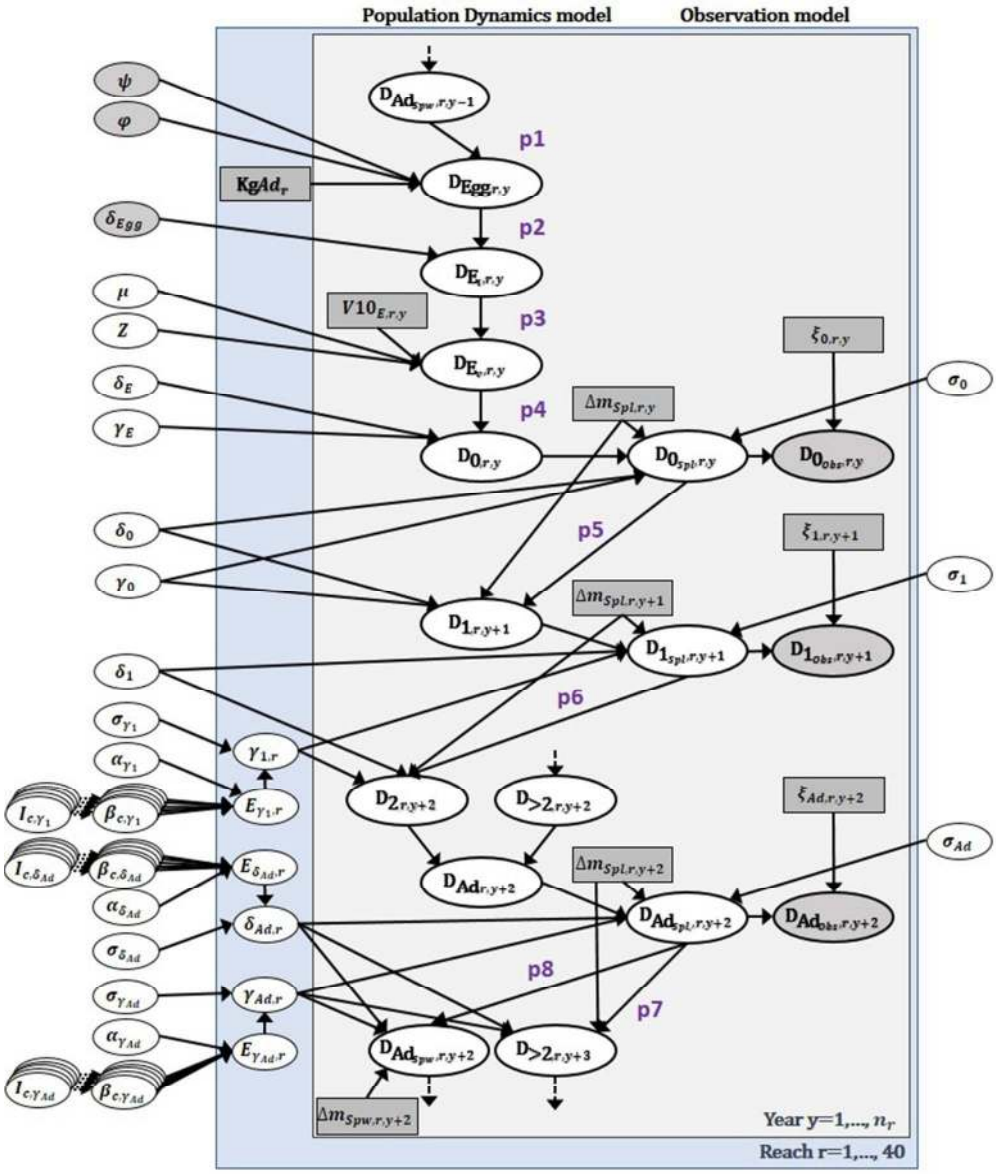

Fig. 3. Directed acyclic graph for the brown trout population dynamics model presented in Fig. 1. Variables represented in ellipses were defined by a probability distribution. White ellipses are non-observed variables; shaded ellipses are data. Shaded boxes represent fixed constant or calculated covariates. Solid-line arrows represent stochastic transitions; dotted-line arrows represent deterministic links (including age-stage transitions, structuring the life-cycle). The number of each process (p1 – p8; detailed in Appendix A) is added.

200x237mm (96 x 96 DPI)

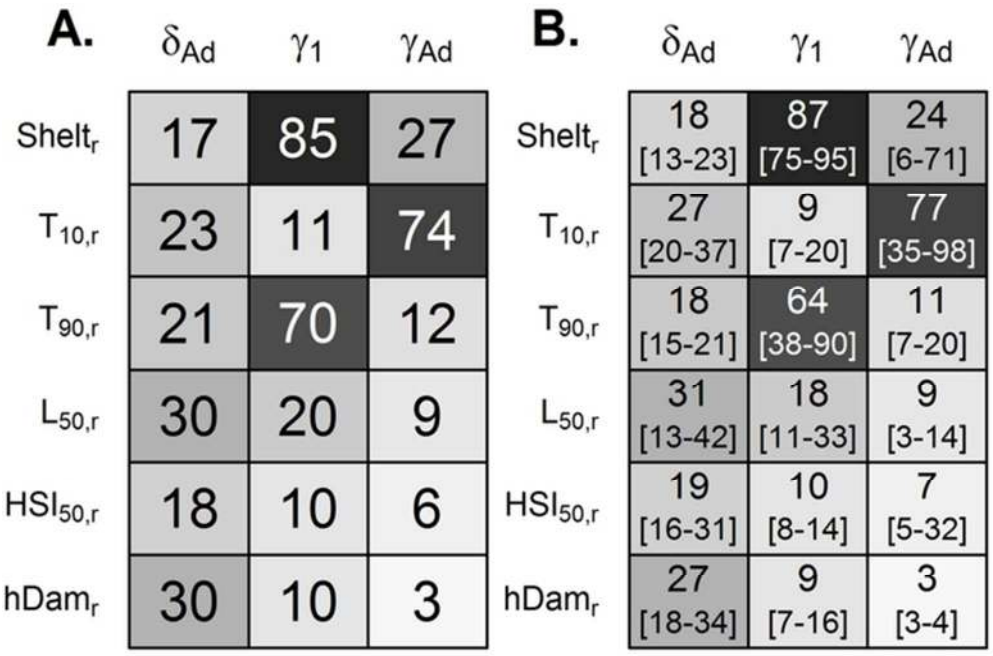

Fig. 4. Posterior frequency of inclusion (in %) of the effect of the 6 studied reach characteristics (rows) on the 3 mortality rates (columns). Table A shows the results of the model for the 40 reaches. Table B summarizes the results of the leave-one-out deletion test, giving median [range] values for posterior frequency of inclusion. Gray scale is associated with the posterior frequency of inclusion.

59x39mm (300 x 300 DPI)

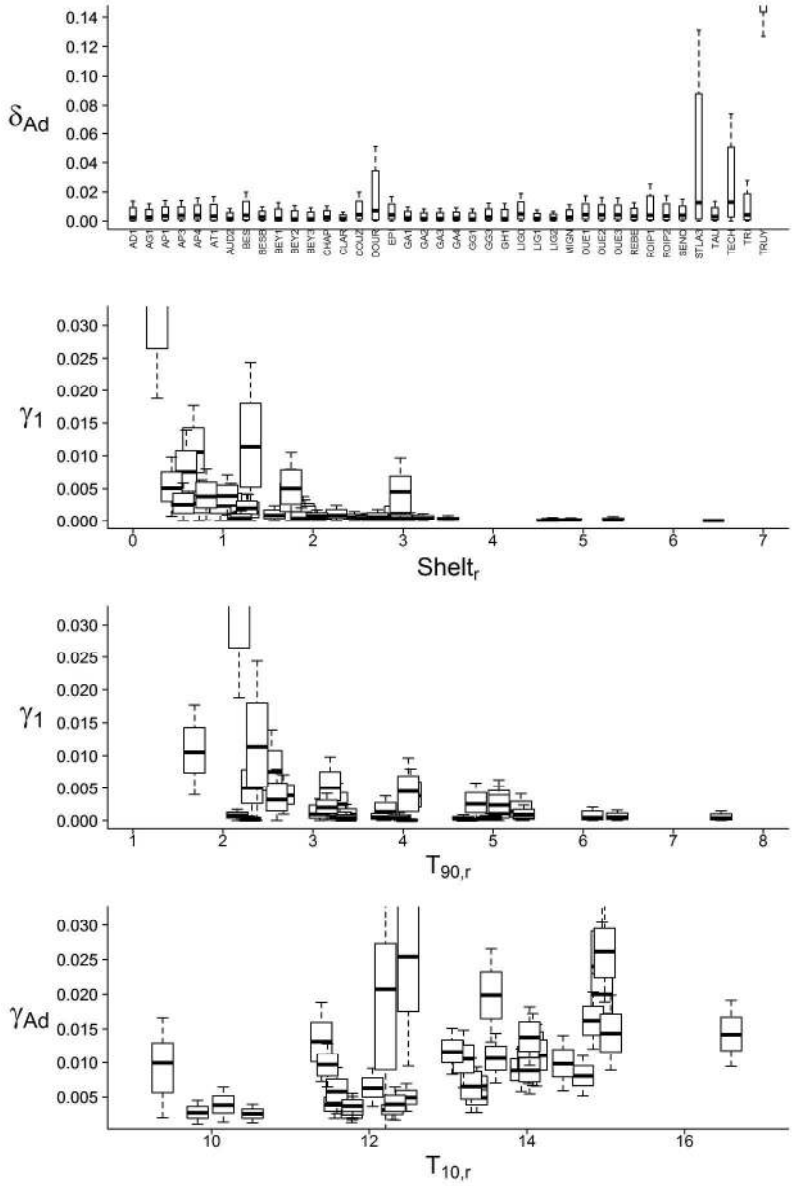

Fig. 5. Marginal posterior distributions of density-independent (δ_{Ad}) and density-dependent (γ_1 and γ_{Ad}) mortality rates modeled by a hierarchical structure for the 40 reaches. The 1st row shows the distribution of δ_{Ad}, which could not be explained by reach characteristics. The 2nd to 5th rows show change in density-dependent mortality distribution (γ_1 and γ_{Ad}) with shelter availability and inter-annual mean of percentile of water temperatures (T_{10} and T_{90}) as covariates.

239x359mm (300 x 300 DPI)

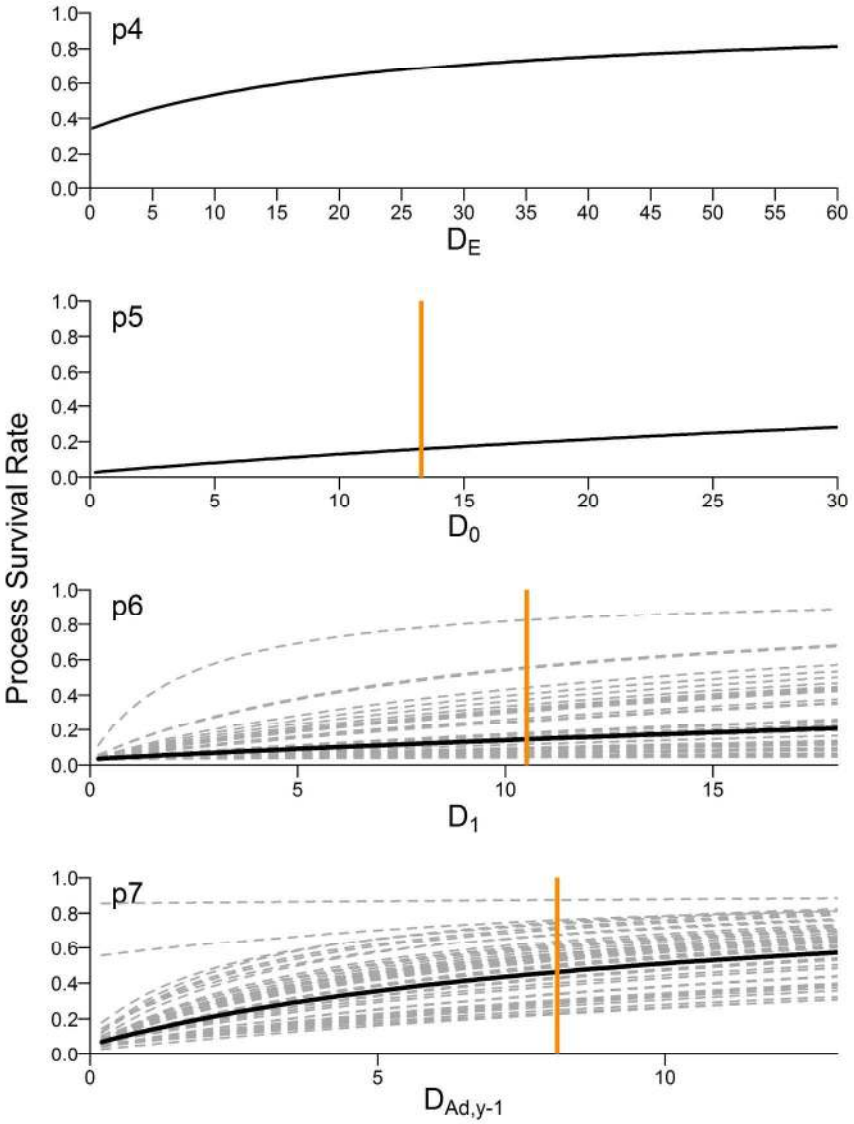

Fig. 6. Total mortality for the processes describing natural mortality between successive age-stages (p4, p5, p6 and p7) for total process duration (respectively, 2, 10, 12 and 12 months). When inter-reach variation in at least one mortality rate (δ_k or γ_k) was detected for age-stage k, fitted relations for the 40 reaches are presented (dashed gray lines) along with the mean expected relation (solid line). A vertical line is drawn at mean observed densities for 0+, 1+and adults (densities were never observed at emergence); upper limits of x-axes correspond to the 90th percentile of observed densities. Mortality from egg to emergent fry is not represented here, as mortality rates were not fitted but taken from the literature.

199x266mm (300 x 300 DPI)

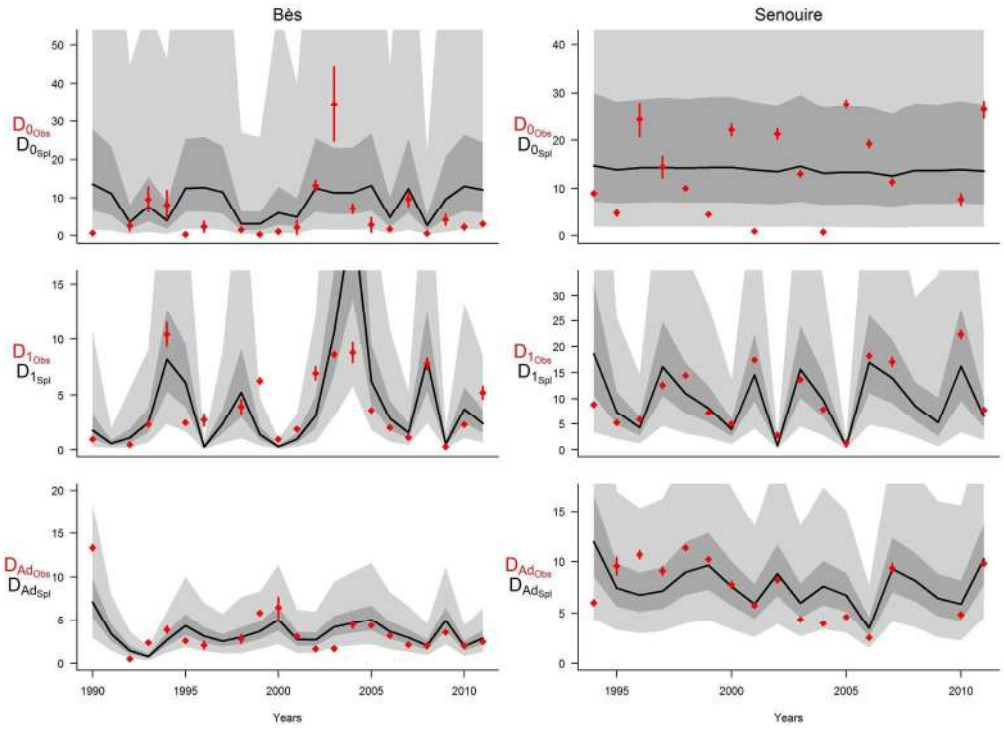

Fig. 7. Time series of observed and predicted densities of 0+, 1+ and adult brown trout in 2 reaches (Bes and Senouire; columns). Points represent observed densities, associated with observation uncertainty (vertical lines). The black line shows the mean estimate of each year's predicted density. The shaded areas show the 50% and 95% confidence intervals for the predicted densities, when process error is considered.

179x129mm (300 x 300 DPI)

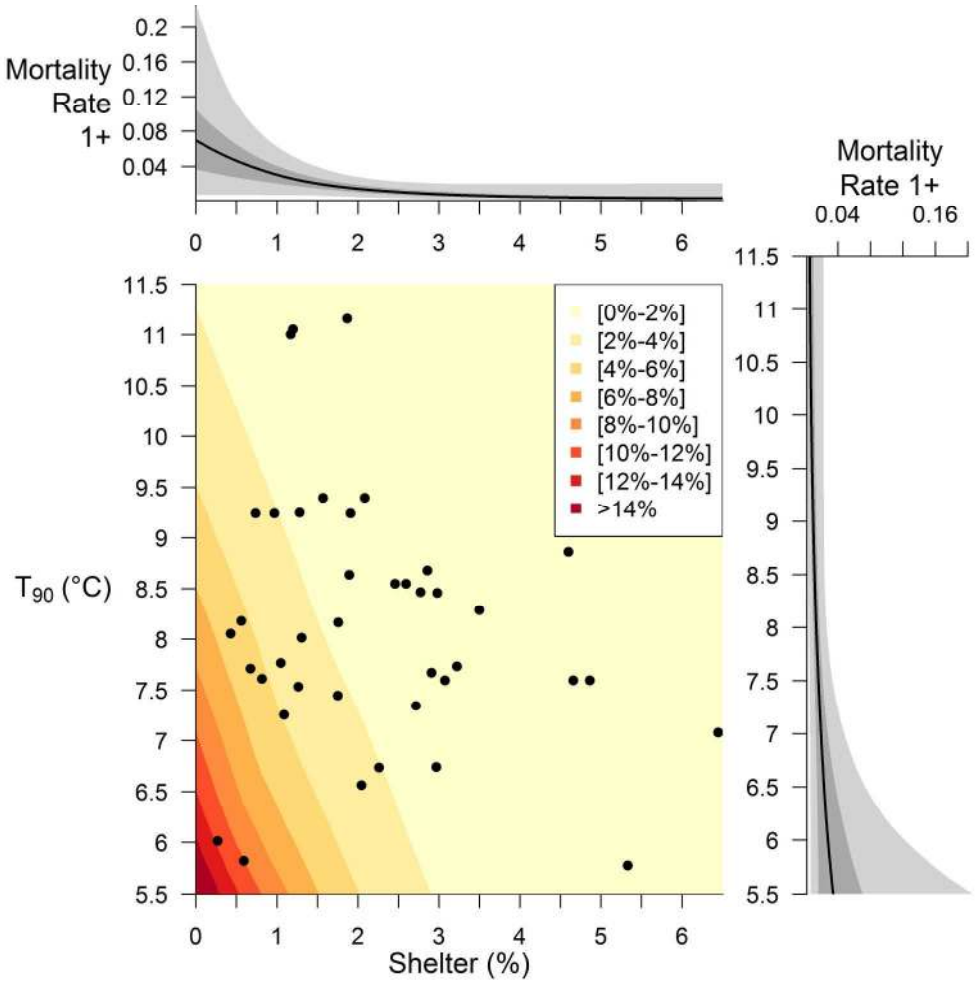

Fig. 8. Prediction of monthly mortality in 1+ depending on shelter availability (x-axis) and inter-annual mean of a percentile of water temperatures (T_{90}) (y-axis). Black dots show the characteristics of reaches considered in this paper. Marginal relations are shown in upper and right sub-panels (shaded areas show 50% and 95% confidence intervals). Monthly mortality was computed by considering both density-independent and density-dependent mortality and for mean initial densities (10.5 ind.100m^{-2} for 1+ and 8.1 ind.100m^{-2} for adults).

199x199mm (300 x 300 DPI)

Appendix A: Detailed modeling of the life-cycle

A1. Calculation of the BH equation

Change in D_k (density of age-stage k) was modeled by 1-month time steps. Mortality processes were described by the alternative formulation of the Beverton and Holt (1957) relationship.

Monthly per capita mortality rate (PCMR) was considered for density-independent mortality δ_m, density-dependent mortality γ_m and population density D_m ($D_m = {N_m}/{S}$, S being the total studied area).

(A1.1) $$\frac{1}{N_m}.\frac{dN_m}{dm} = -\delta_m - \gamma_m.D_m = -\delta_m - \frac{\gamma_m}{S}.N_m$$

Simple algebra on eq. (A1.1) leads to:

$$\leftrightarrow \frac{dN_m}{N_m + \frac{\gamma_m}{S.\delta_m}.{N_m}^2} = -\delta_m.dm$$

(A1.2) $$\leftrightarrow \frac{dN_m}{N_m} - \frac{dN_m}{\frac{\delta_m.S}{\gamma_m} + N_m} = -\delta_m.dm \quad \text{(by the method of partial fractions)}$$

Assuming δ_m and γ_m to be constant during the considered period, (A1.2) can be integrated from m_0 to m_1 ($m_1 = m_0 + \Delta m$):

$$\int_{N=N_{m_0}}^{N=N_{m_1}} \frac{dN_m}{N_m} - \int_{N=N_{m_0}}^{N=N_{m_1}} \frac{dN_m}{\frac{\delta.S}{\gamma} + N_m} = -\int_{m=m_0}^{m=m_1} \delta.dm$$

$$\leftrightarrow \ln(N_{m_1}) - \ln(N_{m_0}) - \left[\ln(\frac{\delta.S}{\gamma} + N_{m_1}) - \ln(\frac{\delta.S}{\gamma} + N_{m_0})\right] = -\delta.\Delta m \quad (as\ \frac{\delta.S}{\gamma} > 0)$$

$$\leftrightarrow \frac{N_{m_1}}{\frac{\delta.S}{\gamma} + N_{m_1}} = \frac{N_{m_0}}{\frac{\delta.S}{\gamma} + N_{m_0}}.e^{-\delta.\Delta m}$$

$$\leftrightarrow \frac{1}{N_{m_1}} = \frac{\gamma}{\delta.S}\left[\frac{\frac{\delta.S}{\gamma} + N_{m_0}.(1 - e^{-\delta.\Delta m})}{N_{m_0}.e^{-\delta.\Delta m}}\right]$$

$$\leftrightarrow N_{m_1} = \frac{N_{m_0}}{e^{\delta.\Delta m} + \frac{\gamma}{\delta.S}.(e^{\delta.\Delta m} - 1).N_{m_0}}$$

(A1.3) $$\leftrightarrow D_{m_1} = \frac{D_{m_0}}{e^{\delta.\Delta m} + \frac{\gamma}{\delta}.(e^{\delta.\Delta m}-1).D_{m_0}}$$

This relation (A1.3) hereafter denoted $D_{m_1} = BH(D_{m_0}, \delta, \gamma, \Delta m)$ is an alternative formulation of the Beverton-Holt stock recruitment relation with slope at the origin α and maximum asymptotic recruitment (or carrying capacity of the river) β:

(A1.4) $$\begin{cases} N_{\Delta m} = \frac{\alpha.N_{m_0}}{1+\alpha.\beta.N_{m_0}} \\ \alpha = e^{-\delta.\Delta m} \\ \beta = \frac{1}{\frac{\gamma}{\delta}(e^{\delta.\Delta m}-1)} \end{cases}$$

The model assumed constant mortality throughout a given age-stage k. Equation (A1.3) can relate densities of successive age-stages by considering the duration of the whole age-stage Δm_k:

$$D_{k+1} = BH(D_k, \delta_k, \gamma_k, \Delta m_k)$$

It could also be used to express intermediate densities within a given age-stage k (from m_0 to $m_0 + \Delta m$):

$$D_{k,m_0+\Delta m} = BH(D_{k,m_0}, \delta_k, \gamma_k, \Delta m)$$

A2. Detailed life-cycle

We detail here the equations describing all steps of the brown trout life-cycle presented in (**Fig. 2**). These processes are associated with process errors taking account of unpredictable between-year variations around the expected process, as presented in the Methods section. For the sake of clarity, we did not index densities with the year y and the reach r considered (D_k being a simplification of $D_{k,y,r}$). Full indexing appears on **Fig. 3**.

Spawning (p1)

Density of spawning adults $D_{Ad_{Spw}}$ in December (Elliott 1994) was multiplied by the brown trout sex-ratio φ, number of eggs per kg of females ψ and the weight (in kg) of adult brown trout $\mathrm{Kg_{Ad,r}}$ to express the density of produced eggs $\mathrm{D_{Egg}}$.

(Eq. A2.1) $$D_{Egg} = D_{Ad_{Spw}}.\varphi.\psi.Kg_{Ad,r}$$

As we did not have local information on spawning processes for all reaches, previous studies on French trout populations were used to obtain global estimates for φ and ψ. Their prior distributions were informative and centered on estimates found in the literature for the 3 parameters (**Table 2**). $Kg_{Ad,r}$ was given in all reaches r by field measurements (inter-annual median of measured weights).

Under-gravel egg mortality (p2)

We then assumed that no density-dependent mortality occurred during incubation and that emergence started in March (Gouraud et al. 2014). Initial densities of emergent fry D_{E_i} were then modeled assuming only density-independent mortality δ_{Egg} operating on D_{Egg} for 3 months.

(Eq. A2.2) $$D_{E_i} = BH(D_{Egg}, \delta_{Egg}, \gamma_{Egg} = 0, \Delta m_{Egg} = 3)$$

Again, we did not have local information on monthly under-gravel mortality for all reaches, and we used a global informative prior for δ_{Egg} (**Table 2**), consistent with the observed survival rate of 90% for the whole period (Bardonnet and Prévost 1994).

Abiotic mortality during emergence: flow velocity (p3)

Emergence lasts up to 2 months (Elliott 1994), grouping together emergence in itself and early post-emergence, which are both sensitive. During emergence, fry mortality occurs when flow velocity becomes too high (Heggenes and Traaen 1988; Armstrong et al. 2003). The influence of flow velocity was then modeled as an excess-mortality rate μ, operating when $V_{10,E}$ (flow velocity for more than 10% of the time during emergence) was higher than a threshold Z (in $m.s^{-1}$):

(Eq. A2.3) $$\begin{cases} D_{E_v} = D_{E_i} & if\ V_{10,r,E} < Z \\ D_{E_v} = D_{E_i}.(1-\mu) & if\ V_{10,r,E} \geq Z \end{cases}$$

As flow velocity has the same implications everywhere, we assumed the process was operating similarly in all reaches: parameters μ and Z were therefore estimated globally.

Prior distributions for these parameters and all the following were weakly informative (**Table 3**).

Mortality process during emergence (p4)

Emergence is also characterized by high mortality while the young trout establish feeding territories (Elliott 1994). We modeled natural fry mortality on specific mortality rates for these 2 months:

(Eq. A2.4) $$D_0 = BH(D_{E_v}, \delta_E, \gamma_E, \Delta m_E = 2)$$

Available data (summer samplings) did not allow precise estimation of inter-reach variability in mortality during emergence. To ensure the convergence of the model, we had to estimate δ_E and γ_E globally. Inter-year variations in emergence mortality (mostly linked to abiotic conditions) are known to be high (e.g., Hayes et al. 2010; Lobón-Cerviá et al. 2012). We therefore assumed, for this first step of modeling, that inter-reach variations were comparatively negligible.

Mortality process during the end of the first year (Age-stage 0; p5)

After this critical period, we assumed constant monthly mortality (δ_0 and γ_0) during the last 10 months of the first year of life, (age-stage 0 in **Fig. 2**). We modeled density for an intermediate state of age-stage 0, $D_{0_{Spl}}$, at the month of sampling (Δm_{Spl} months after the beginning of the age-stage). This intermediate state was used to compute the likelihood of the model.

(Eq. A2.5) $$\begin{cases} D_{0_{Spl}} = BH(D_0, \delta_0, \gamma_0, \Delta m = \Delta m_{Spl}) \\ D_1 = BH(D_{0_{Spl}}, \delta_0, \gamma_0, \Delta m = 12 - \Delta m_{Spl}) \end{cases}$$

Inter-reach variation in mortality during age-stage 0 were not identified by our preliminary analyses (**Appendix B**). Those parameters were therefore estimated globally.

Mortality process during the second year of life (Age-stage 1; p6)

Trout from age-stage 1 surviving the 2nd year of life become 2+ trout (age-stage 2 being a subset of the adult age-stage):

(Eq. A2.6) $$\begin{cases} D_{1_{Spl}} = BH(D_1, \delta_1, \gamma_{1,\mathrm{r}}, \Delta m = \Delta m_{Spl}) \\ D_2 = BH(D_{1_{Spl}}, \delta_1, \gamma_{1,r}, \Delta m = 12 - \Delta m_{Spl}) \end{cases}$$

Preliminary analyses (**Appendix B**) revealed inter-reach variations in density-dependent mortality γ_1 but not density-independent mortality δ_1. Thus, a hierarchical setting was used for γ_1 while δ_1 was estimated globally.

Adult mortality (p7)

The adult age-stage combined fish of several ages (2+ and older).

(Eq. A2.7)
$$\begin{cases} D_{Ad} = D_2 + D_{>2} \\ \mathrm{D}_{Ad_{Spl}} = BH\left(D_{Ad}, \delta_{Ad,r}, \gamma_{Ad,r}, \Delta m = \Delta m_{Spl}\right) \\ D_{>2} = BH(\mathrm{D}_{Ad_{Spl}}, \delta_{Ad,r}, \gamma_{Ad,r}, \Delta m = 12 - \Delta m_{Spl}) \end{cases}$$

Preliminary analyses (**Appendix B**) revealed inter-reach variations in both density-dependent mortality γ_{Ad} and density-independent mortality δ_{Ad}. Thus, a hierarchical setting was used for these parameters.

Spawning adults (p8)

Finally, the density of spawning adults in December was related to the mortality of adults from sampling to spawning (Δm_{Spw} months after sampling):

(Eq. A2.8)
$$DAd_{Spw} = BH(\mathrm{D}_{Ad_{Spl}}, \delta_{Ad}, \gamma_{Ad}, \Delta m = \Delta m_{Spw})$$

A3. Appendix A: References

Armstrong, J. D., Kemp, P. S., Kennedy, G. J. A., Ladle, M., and Milner, N. J. 2003. Habitat requirements of Atlantic salmon and brown trout in rivers and streams. Fish. Res. **62**(2): 143-170. doi:doi:10.1016/S0165-7836(02)00160-1.

Bardonnet, A., and Prévost, E. 1994. Survie sous gravier de la truite (*Salmo trutta*) dans un affluent du Scorff.

Beverton, R. J. H., and Holt, S. J. 1957. On the dynamics of exploited fish populations. London, UK, Chapman & Hall.

Elliott, J. M. 1994. Quantitative ecology and the brown trout. Oxford GBR, Oxford University Press.

Gouraud, V., Baran, P., Bardonnet, A., Beaufrère, C., Capra, H., Caudron, A., Delacoste, M., Lescaux, J. M., Naura, M., Ovidio, M., Poulet, N., Tissot, L., Sebaston, C., and Baglinière, J.-L. 2014. Sur quelles connaissances se baser pour évaluer l'état de santé

107 des populations de truite commune (*Salmo trutta*)? Hydroécologie Appliquée: 1-28.
108 doi:10.1051/hydro/2014001.
109 Hayes, J. W., Olsen, D. A., and Hay, J. 2010. The influence of natural variation in discharge
110 on juvenile brown trout population dynamics in a nursery tributary of the Motueka
111 River, New Zealand. New Zeal. J. Mar. Fresh. **44**(4): 247-269.
112 doi:10.1080/00288330.2010.509905.
113 Heggenes, J., and Traaen, T. 1988. Downstream migration and critical water velocities in
114 stream channels for fry of four salmonid species. J. Fish Biol. **32**(5): 717-727.
115 doi:10.1111/j.1095-8649.1988.tb05412.x.
116 Lobón-Cerviá, J., Budy, P., and Mortensen, E. 2012. Patterns of natural mortality in stream-
117 living brown trout (*Salmo trutta*). Freshw. Biol. **57**(3): 575-588. doi:10.1111/j.1365-
118 2427.2011.02726.x.

119